Journal of Computational Physics 229 (2010) 1–31

Contents lists available at ScienceDirect

Journal of Computational Physics

journal homepage: www.elsevier.com/locate/jcp

Test models for improving filtering with model errors through stochastic parameter estimation

B. Gershgorin [a], J. Harlim [b,*], A.J. Majda [a]

[a] Department of Mathematics and Center for Atmosphere and Ocean Science, Courant Institute of Mathematical Sciences, New York University, NY 10012, United States
[b] Department of Mathematics, North Carolina State University, NC 27695, United States

ARTICLE INFO

Article history:
Received 13 April 2009
Received in revised form 17 August 2009
Accepted 21 August 2009
Available online 29 August 2009

Keywords:
Stochastic parameter estimation
Kalman filter
Filtering turbulence
Data assimilation
Model error

ABSTRACT

The filtering skill for turbulent signals from nature is often limited by model errors created by utilizing an imperfect model for filtering. Updating the parameters in the imperfect model through stochastic parameter estimation is one way to increase filtering skill and model performance. Here a suite of stringent test models for filtering with stochastic parameter estimation is developed based on the Stochastic Parameterization Extended Kalman Filter (SPEKF). These new SPEKF-algorithms systematically correct both multiplicative and additive biases and involve exact formulas for propagating the mean and covariance including the parameters in the test model. A comprehensive study is presented of robust parameter regimes for increasing filtering skill through stochastic parameter estimation for turbulent signals as the observation time and observation noise are varied and even when the forcing is incorrectly specified. The results here provide useful guidelines for filtering turbulent signals in more complex systems with significant model errors.

1. Introduction

Filtering is the process of obtaining the best statistical estimate of a natural system from partial observations of the signal from nature. In many contemporary applications in science and engineering, real time filtering of a turbulent signal from nature involving many degrees of freedom is needed to make accurate predictions of the future state. This is obviously a problem with significant practical impact. Important contemporary examples involve the real time filtering and prediction of weather and climate as well as the spread of hazardous plumes or pollutants. A major difficulty in accurate filtering of noisy turbulent signals with many degrees of freedom is model error [1]; the fact that the signal from nature is processed through an imperfect model where important physical processes are parameterized due to inadequate numerical resolution or incomplete physical understanding. Under these circumstances it is natural to devise strategies for parameter estimation to cope with model errors to improve filtering skill with model errors [2–9].

The simplest contemporary strategy to cope with model errors for filtering with an imperfect model nonlinear dynamical system depending on parameters, λ,

$$\frac{du}{dt} = F(u, \lambda) \tag{1}$$

is to augment the state variable u, by the parameters λ, and adjoin an approximate dynamical equation for the parameters

* Corresponding author.
E-mail address: jharlim@ncsu.edu (J. Harlim).

0021-9991/$ - see front matter © 2009 Elsevier Inc. All rights reserved.
doi:10.1016/j.jcp.2009.08.019

$$\frac{d\lambda}{dt} = g(\lambda). \tag{2}$$

The right hand side of (2) is often chosen on an ad-hoc basis as $g(\lambda) \equiv 0$ or white noise forcing with a small variance [10,11]. The partial observations of the signal from nature are often processed by an Extended Kalman Filter (EKF, see [12–14]) applied to the augmented system in (1) and (2) where the parameters λ are estimated adaptively from these partial observations. Note that even if the original model in (1) is linear, it readily can have nonlinear dependence on the parameters λ so typically an EKF involving the linear tangent approximation and Kalman filtering is needed for parameter estimation in this standard case. Some recent applications of these and similar ideas to complex nonlinear dynamical system can be found in [2–4,6,7].

The topic of the present paper is the development of stringent test models for filtering turbulent signals from nature in the presence of significant model error and the improvement of filtering and skill through systematic stochastic parameter estimation. Here we develop a suite of exact Stochastic Parameterization Extended Kalman Filters (SPEKF) for stochastic parameter estimation and filtering in these test models following recent work of two of the authors [15,16] for filtering slow–fast systems. The test models include both additive and multiplicative bias corrections and their exactly solvable features yield important new guidelines for stochastic parameter estimation. Results below include comprehensive understanding of robust regimes for improved filtering skill with stochastic parameter estimation as well as delineating regimes of parameters with poor skill as different aspects of the observation time, observation noise variance, and the properties of the prototype signal from nature are varied. The exact statistical formulas with exponential growth in time developed in Section 2 below also point toward the potential lack of skill of EKF for stochastic parameter estimation.

1.1. Overview of the test models

In the test models here, the signals from nature are assumed to be given by the solution of the time dependent complex scalar Langevin equation

$$\frac{du(t)}{dt} = -\gamma(t)u(t) + \mathrm{i}\omega u(t) + \sigma\dot{W}(t) + f(t), \tag{3}$$

where $\dot{W}(t)$ is complex white noise and $f(t)$ is a prescribed external forcing. To generate significant model error as well as to mimic intermittent chaotic instability as often occurs in nature, we allow $\gamma(t)$ to switch between stable ($\gamma > 0$) and unstable ($\gamma < 0$) regimes according to a two-state Markov jump process. Here we regard $u(t)$ as representing one of the modes from nature in a turbulent signal as is often done in turbulence models [17–20], and the switching process can mimic physical features such as intermittent baroclinic instability [21]. As often occurs in practice, we assume that the switching process details are not known and only averaged properties are modeled. Thus, the Mean Stochastic Model (MSM) with significant model error given by

$$\frac{du(t)}{dt} = -\bar{\gamma}u(t) + \mathrm{i}\omega u(t) + \sigma\dot{W}(t) + \tilde{f}(t) \tag{4}$$

is utilized for filtering; here $\bar{\gamma} > 0$ is an average damping constant and $\tilde{f}(t)$ is possibly an incorrectly specified forcing. The SPEKF filters for stochastic parameter estimation are developed below in the context of true signal arising from (3) with the basic imperfect models developed in (4). The context of (3) and (4) provides a stringent test problem for improving filtering skill through stochastic parameter estimation which we develop below. In Section 2, we introduce the family of stochastic parameter estimation models and develop exactly solvable first and second order statistics for these models following [15,16]. Details of the model in (3) for true signal are described in Section 3 while a comprehensive study of the filtering skill through stochastic parameter estimation is presented in Section 4. In particular, Section 4 includes discussion of robustness and sensitivity to stochastic parameters in both the forced and unforced cases as well as learning the forcing from the filter process when the forcing is specified incorrectly. Section 5 contains concluding discussion, which indicates the fashion in which the stochastic estimation models, developed here, might be directly applied to turbulent dynamical systems with many degrees of freedom [22–25] as developed in a companion paper [26].

2. Exactly solvable test models for stochastic parameter estimation

2.1. Combined model

We consider a stochastic model for the evolution of state variable $u(t)$ together with *combined* additive, $b(t)$, and multiplicative, $\gamma(t)$, bias correction terms:

$$\begin{aligned}
\frac{du(t)}{dt} &= (-\gamma(t) + \mathrm{i}\omega)u(t) + b(t) + f(t) + \sigma\dot{W}(t),\\
\frac{db(t)}{dt} &= (-\gamma_b + \mathrm{i}\omega_b)(b(t) - \hat{b}) + \sigma_b\dot{W}_b(t),\\
\frac{d\gamma(t)}{dt} &= -d_\gamma(\gamma(t) - \hat{\gamma}) + \sigma_\gamma\dot{W}_\gamma(t)
\end{aligned} \tag{5}$$

for improving filtering with model errors. Here, ω is the oscillation frequency of $u(t)$, $f(t)$ is an external forcing, and σ characterizes the strength of the white noise forcing $\dot{W}(t)$. Also, parameters γ_b and d_γ represent the damping and parameters σ_b and σ_γ represent the strength of the white noise forcing of the additive and multiplicative bias correction terms, respectively. The stationary mean bias correction values of $b(t)$ and $\gamma(t)$ are given by $\hat{b}$ and $\hat{\gamma}$, correspondingly; and the frequency of the additive noise is denoted as ω_b. Note that the white noise $\dot{W}_\gamma(t)$ is real valued while the white noises $\dot{W}(t)$ and $\dot{W}_b(t)$ are complex valued and their real and imaginary parts are independent real valued white noises. It is important to realize that the parameters of the state variable $u(t)$ come from the characteristics of the physical system, which is modeled by the first equation in (5). On the other hand, parameters of $b(t)$ and $\gamma(t)$, $\{\gamma_b, \omega_b, \sigma_b, d_\gamma, \sigma_\gamma\}$, are introduced in the model and, in principle, cannot be directly obtained from the characteristics of the physical system. One of the goals of this paper is to study how the results of the filtering are sensitive to wide variations of these parameters, and to obtain some insights on how to choose them. In our numerical study, we will consider an oscillatory external forcing

$$f(t) = A_f e^{i\omega_f t}, \tag{6}$$

however, any arbitrary smooth enough function $f(t)$ can be chosen. As a special case, we will also study the unforced system with $f(t) \equiv 0$.

System (5) is considered with the initial values

$$\begin{aligned} u(t_0) &= u_0, \\ b(t_0) &= b_0, \\ \gamma(t_0) &= \gamma_0, \end{aligned}$$

which are independent Gaussian random variables with the known statistics: $\langle u_0 \rangle$, $\langle \gamma_0 \rangle$, $\langle b_0 \rangle$, $Var(u_0)$,, $Var(\gamma_0)$, $Var(b_0)$, $Cov(u_0, u_0^*)$, $Cov(u_0, \gamma_0)$, $Cov(u_0, b_0)$, $Cov(u_0, b_0^*)$.

2.2. Additive and multiplicative models

We consider two special cases of the combined model (5): The *additive model* when we have only the additive bias correction

$$\begin{aligned} \frac{du(t)}{dt} &= (-\bar{d} + i\omega)u(t) + b(t) + f(t) + \sigma\dot{W}(t), \\ \frac{db(t)}{dt} &= (-\gamma_b + i\omega_b)(b(t) - \hat{b}) + \sigma_b\dot{W}_b(t), \end{aligned} \tag{7}$$

and the *multiplicative model* when we have only multiplicative bias correction

$$\begin{aligned} \frac{du(t)}{dt} &= (-\gamma(t) + i\omega)u(t) + f(t) + \sigma\dot{W}(t), \\ \frac{d\gamma(t)}{dt} &= -d_\gamma(\gamma(t) - \hat{\gamma}) + \sigma_\gamma\dot{W}_\gamma(t), \end{aligned} \tag{8}$$

where $\bar{d}$ is the mean value of the damping. Note that the model with additive bias correction only, (7), is linear. These two special cases are designed for the purpose of comparison with the combined model. Moreover, studying the filter performance based on the combined model as well as on the multiplicative and additive models will help us understand which component of the bias corrections is more important depending on the physical properties of the system, such as its damping and external forcing. We will find out that there are exceptional situations when the multiplicative model performs slightly better than the combined model and there are situations when the additive model is as good as the combined model. The former situation occurs because of sampling error in the additive bias term, $b(t)$, when the external forcing is specified correctly. However, we will demonstrate via extensive numerical study that the combined model is the most robust to the variations of parameters and, therefore, it should be the method of choice when there is no additional information that indicates in advance that either multiplicative or additive models is better in a particular situation.

2.3. Path-wise solution

Here, we present the exact path-wise solution for system (5). Additive and multiplicative bias correction terms, $b(t)$ and $\gamma(t)$, should be found first since the state variable $u(t)$ depends on them

$$b(t) = \hat{b} + (b_0 - \hat{b})e^{\lambda_b(t-t_0)} + \sigma_b \int_{t_0}^{t} e^{\lambda_b(t-s)} dW_b(s), \tag{9}$$

$$\gamma(t) = \hat{\gamma} + (\gamma_0 - \hat{\gamma})e^{-d_\gamma(t-t_0)} + \sigma_\gamma \int_{t_0}^{t} e^{-d_\gamma(t-s)} dW_\gamma(s), \tag{10}$$

where $\lambda_b = -\gamma_b + i\omega_b$, and $\hat{b}$ and $\hat{\gamma}$ are the stationary bias correction values of $b(t)$ and $\gamma(t)$. Now, we introduce new notations

$$\hat{\lambda} = -\hat{\gamma} + i\omega,$$
$$J(s,t) = \int_s^t (\gamma(s') - \hat{\gamma})ds'.$$

Then, using these notation, we find the solution for $u(t)$

$$u(t) = e^{-J(t_0,t)+\hat{\lambda}(t-t_0)}u_0 + \int_{t_0}^t (b(s)+f(s))e^{-J(s,t)+\hat{\lambda}(s-t_0)}ds + \sigma\int_{t_0}^t e^{-J(s,t)+\hat{\lambda}(s-t_0)}dW(s). \tag{11}$$

2.4. Exact statistics for nonlinear combined model

In this section, we show how to find the first and second order statistics of the combined model (5). These statistics are the main formulas for updating the prior statistics in the Kalman filter. Note that the first equation in (5) is nonlinear and, therefore, in general, Gaussian initial values at $t = t_0$ will not stay Gaussian for $t > t_0$. However, the special structure of the first equation in (5) allows us to find exact analytical formulas for the first and second (and, in principle, any) order statistics. The technique of obtaining the first and second order statistics for the kind of nonlinearity used in system (5) was already studied in [15,16]. Here, we will follow the same procedure outlining the most interesting and important points. In principle, these formulas follow from general mathematical formulas for conditionally Gaussian processes [27]; however, the detailed properties of the explicit formulas are of interest here.

We start with the statistics of $b(t)$ and $\gamma(t)$. The second and third equations in (5) are linear SDEs and their solutions are Gaussian given Gaussian initial data. The mean and covariance of $b(t)$ and $\gamma(t)$ are the following

$$\langle b(t)\rangle = \hat{b} + (\langle b_0\rangle - \hat{b})e^{\lambda_b(t-t_0)}, \tag{12}$$

$$\langle \gamma(t)\rangle = \hat{\gamma} + (\langle \gamma_0\rangle - \hat{\gamma})e^{-d_\gamma(t-t_0)}, \tag{13}$$

$$Var(b(t)) = Var(b_0)e^{-2\gamma_b(t-t_0)} + \frac{\sigma_b^2}{2\gamma_b}(1 - e^{-2\gamma_b(t-t_0)}), \tag{14}$$

$$Var(\gamma(t)) = Var(\gamma_0)e^{-2d_\gamma(t-t_0)} + \frac{\sigma_\gamma^2}{2d_\gamma}(1 - e^{-2d_\gamma(t-t_0)}), \tag{15}$$

$$Cov(b(t), b(t)^*) = Cov(b_0, b_0^*)e^{2\lambda_b(t-t_0)}, \tag{16}$$

$$Cov(b(t), \gamma(t)) = e^{(-d_\gamma+\lambda_b)(t-t_0)}Cov(b_0, \gamma_0). \tag{17}$$

Next, we find the mean $\langle u(t)\rangle$ using Eq. (11)

$$\langle u(t)\rangle = e^{\hat{\lambda}(t-t_0)}\langle u_0 e^{-J(t_0,t)}\rangle + \int_{t_0}^t e^{\hat{\lambda}(t-s)}\langle b(s)e^{-J(s,t)}\rangle ds + \int_{t_0}^t e^{\hat{\lambda}(t-s)}f(s)\langle e^{-J(s,t)}\rangle ds. \tag{18}$$

Following [15,16], the averages in the RHS of Eq. (18) can be computed using the characteristic function of Gaussian random process $J(s,t)$. Recall that for given complex Gaussian z and real Gaussian x, we have

$$\langle ze^{bx}\rangle = (\langle z\rangle + bCov(z,x))e^{b\langle x\rangle + \frac{b^2}{2}Var(x)}. \tag{19}$$

Note that u_0 and $b(s)$ are Gaussian and so is $J(s,t)$ since it is an integral of Gaussian random process $\gamma(t)$. Applying Eq. (19) to Eq. (18) and then using Eq. (9), we find

$$\begin{aligned}\langle u(t)\rangle = {} & e^{\hat{\lambda}(t-t_0)}(\langle u_0\rangle - Cov(u_0, J(t_0,t)))e^{-\langle J(t_0,t)\rangle + \frac{1}{2}Var(J(t_0,t))} + \int_{t_0}^t e^{\hat{\lambda}(t-s)}(\hat{b} + e^{\lambda_b(s-t_0)}(\langle b_0\rangle - \hat{b} - Cov(b_0, J(s,t))))\\ & \times e^{-\langle J(s,t)\rangle + \frac{1}{2}Var(J(s,t))}ds + \int_{t_0}^t e^{\hat{\lambda}(t-s)}f(s)e^{-\langle J(s,t)\rangle + \frac{1}{2}Var(J(s,t))}ds.\end{aligned} \tag{20}$$

Using the linear property of the covariance, we find

$$Cov(u_0, J(s,t)) = \frac{1}{d_\gamma}\left(e^{-d_\gamma(s-t_0)} - e^{-d_\gamma(t-t_0)}\right)Cov(u_0, \gamma_0),$$
$$Cov(b_0, J(s,t)) = \frac{1}{d_\gamma}(e^{-d_\gamma(s-t_0)} - e^{-d_\gamma(t-t_0)})Cov(b_0, \gamma_0).$$

In order to find $\langle J(s,t)\rangle$, we integrate Eq. (13) to obtain

$$\langle J(s,t)\rangle = \frac{1}{d_\gamma}(e^{-d_\gamma(s-t_0)} - e^{-d_\gamma(t-t_0)})(\langle\gamma_0\rangle - \hat{\gamma}). \tag{21}$$

The variance of $J(s,t)$ can be found using Ito isometry formula [28]

$$\left\langle \left(\int g(t)dW(t) \right)^2 \right\rangle = \int g^2(t)dt,$$

for any deterministic $g(t)$. Then, we obtain

$$Var(J(s,t)) = \frac{1}{d_\gamma^2}(e^{-d_\gamma(s-t_0)} - e^{-d_\gamma(t-t_0)})^2 Var(\gamma_0) - \frac{\sigma_\gamma^2}{d_\gamma^3}[1 + d_\gamma(s-t) + e^{-d_\gamma(s+t-2t_0)} \times (-1 - e^{2d_\gamma(s-t_0)} + \cosh(d_\gamma(s-t)))]. \tag{22}$$

Finally, we find that the mean of $u(t)$ at time t can be expressed in terms of the initial statistics of the system (5) at time t_0. The integrals in the RHS of Eq. (20) can be approximated using the trapezoidal rule,

$$\int_{t_0}^{t} g(s)ds \approx \frac{h}{2}(g(t_0) + g(t)) + h\sum_{j=1}^{N-1} g(t_0 + jh),$$

which gives second order accuracy, where $h = (t - t_0)/N$ is a time step in the equidistant partition of the interval $[t_0, t]$ into N subintervals. In our numerical simulations, we empirically find that $h = 10^{-3}$ insures numerical accuracy. Similarly as in [15,16], we can find the second order statistics of $u(t), \gamma(t)$, and $b(t)$ such as $Var(u(t))$, $Cov(u(t), u^*(t))$, $Cov(u(t), \gamma(t))$, $Cov(u(t), b(t))$, and $Cov(u(t), b^*(t))$. However, since these computations are long, we present them in the Appendix.

Next, we compare the analytically derived statistics of $u(t), b(t)$, and $\gamma(t)$ with their respective averaged values through Monte Carlo simulations. In Fig. 1, the solid line corresponds to the analytically obtained statistics such as Eq. (20) for $\langle u(t)\rangle$ and equations in the Appendix for the second order statistics. On the other hand, circles correspond to the Monte Carlo approximations of the same statistics through the average of Monte Carlo trials using Eqs. (9)–(11). We note excellent agreement between the analytically obtained statistics and their Monte Carlo approximation which gives us high confidence in the validity of the analytic formulas.

2.5. Observability of the combined model

So far, we have shown that the first and second order statistics of the combined model (5) can be found analytically. In principle the same strategy can be used to compute any order statistics. However, for the purpose of using the Stochastic Parameterization Extended Kalman Filter (SPEKF) as in [15,16], we only need the mean and covariance. Also, we can easily reduce the equations for the first and second order statistics to the cases of only multiplicative or only additive bias correction terms. In the former case, we would only have two variables $u(t)$ and $\gamma(t)$. Therefore, we would only compute the statistics that involve only these two variables; and the formulas for these statistics are obtained by setting $b(t) \equiv 0$ in the formulas for the statistics of the combined model. On the other hand, for the case of only additive bias correction terms, we only have the variables $u(t)$ and $b(t)$. We can either find the formulas for the first and second order statistics directly from the original model 5) by setting $\gamma(t) \equiv \hat{\gamma}$, or we can set $\gamma(t) \equiv \hat{\gamma}$ (and, therefore, $J(s,t) \equiv 0$) in the formulas for the first and second order statistics of the combined model stated in Section 2.4 and the Appendix.

Next, we study the observability [29,13,14] of the combined model (5). Since this model is nonlinear, we first linearize it around a mean state

$$u(t) = \bar{u}(t) + \tilde{u}(t),$$

$$b(t) = \bar{b}(t) + \tilde{b}(t),$$

$$\gamma(t) = \bar{\gamma}(t) + \tilde{\gamma}(t).$$

Then, the homogeneous part of the dynamics of the perturbation vector $\widetilde{\mathbf{U}} = (\tilde{u}, \tilde{b}, \tilde{\gamma})^T$ is given by

$$\frac{d\widetilde{\mathbf{U}}}{dt} = A\widetilde{\mathbf{U}}, \tag{23}$$

where the matrix A becomes

$$A = \begin{pmatrix} \lambda & 1 & -\bar{u} \\ 0 & \lambda_b & 0 \\ 0 & 0 & -d_\gamma \end{pmatrix},$$

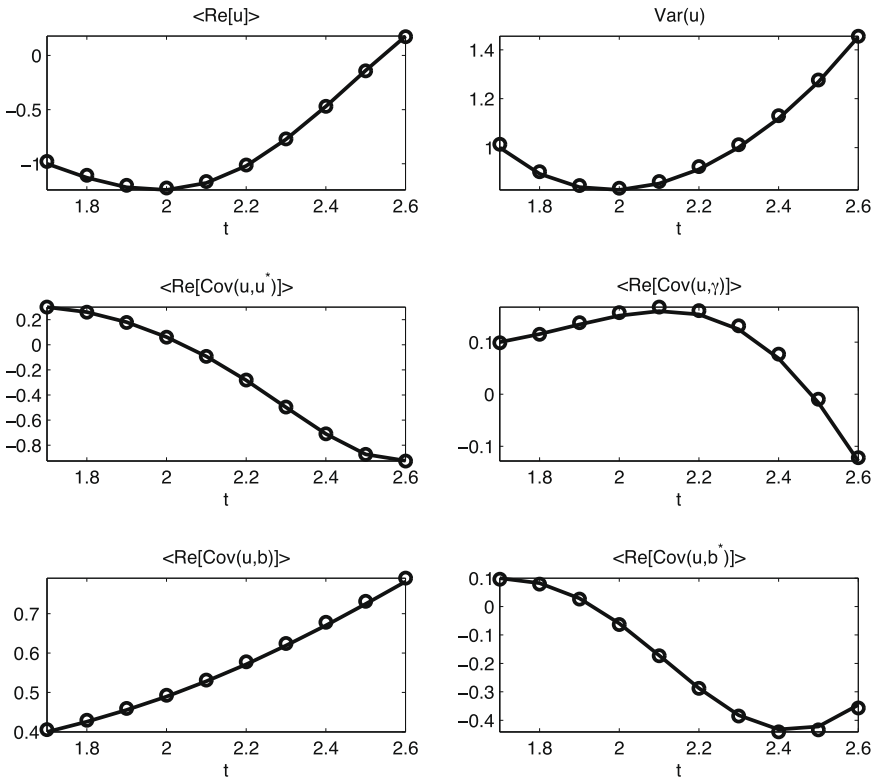

Fig. 1. First and second order statistics of $u(t)$, $b(t)$, and $\gamma(t)$. Solid line corresponds to the analytical formulas for the statistics and circles correspond to Monte Carlo averaging of an emsemble of solutions.

where $\lambda = -\bar{\gamma} + i\omega$. The solution for Eq. (23) is given by

$$\widetilde{\mathbf{U}}(t) = F\widetilde{\mathbf{U}}(t_0),$$

where

$$F = e^{At} = \begin{pmatrix} e^{\lambda t} & \frac{e^{\lambda t} - e^{\lambda_b t}}{\lambda - \lambda_b} & -\bar{u}\frac{e^{\lambda t} - e^{-d_\gamma t}}{d_\gamma + \lambda} \\ 0 & e^{\lambda_b t} & 0 \\ 0 & 0 & e^{-d_\gamma t} \end{pmatrix}.$$

In our study, we only have observations of $u(t)$ but not of $b(t)$ or $\gamma(t)$ since the last two variables are parameters artificially introduced in the model. So the observation, v, is modeled by

$$v = G(u, b, \gamma)^T + \sigma^o, \tag{24}$$

where σ^o is a Gaussian noise with zero mean and variance r^o and

$$G = (1 \quad 0 \quad 0)$$

is the observation operator. Recall that observability [29,12–14] of the linear system, (23) and (24), is associated with the rank of the observability matrix

$$\mathbf{O} = \begin{bmatrix} G \\ GF \\ GF^2 \end{bmatrix}.$$

In our filtering problem, the observability matrix becomes

$$\mathbf{O} = \begin{pmatrix} 1 & 0 & 0 \\ e^{\lambda t} & \frac{e^{\lambda_b t} - e^{\lambda t}}{\lambda - \lambda_b} & -\bar{u}\frac{e^{\lambda t} - e^{-d_\gamma t}}{d_\gamma + \lambda} \\ e^{2\lambda t} & \frac{(e^{\lambda_b t} - e^{\lambda t})^2}{(\lambda - \lambda_b)^2} & -\bar{u}^2\frac{(e^{\lambda t} - e^{-d_\gamma t})^2}{(d_\gamma + \lambda)^2} \end{pmatrix}.$$

Then, the linear system is nonobservable, when the observability matrix is singular, i.e., $\det(\mathbf{O}) = 0$ with

$$\det(\mathbf{O}) = -\bar{u}\frac{(e^{\lambda t} - e^{-d_\gamma t})(e^{\lambda_b t} - e^{\lambda t})}{(d_\gamma + \lambda)(\lambda - \lambda_b)} \times \left(\frac{e^{\lambda_b t} - e^{\lambda t}}{\lambda_b - \lambda} + \bar{u}\frac{e^{\lambda t} - e^{-d_\gamma t}}{d_\gamma + \lambda}\right) = 0. \tag{25}$$

This determinant vanishes for any t if $\bar{u} = 0$ in the case $\lambda \neq \lambda_b$ and $d_\gamma + \lambda \neq 0$. The first term, $\bar{u} = 0$, shows the loss of observability in the multiplicative bias correction term, while the vanishing of the last factor in (25) corresponds to the loss of observability in the additive bias correction term for specific times depending on $\bar{u},\ \lambda_b,\ d_\gamma$. This fact can be easily verified by checking the observability for both the additive and multiplicative models in (7) and (8), respectively.

3. Markov switching models for true signal to be filtered

In this section, we describe a stochastic process that will be used as the true signal for filtering. In particular, we consider a realization of the complex Ornstein–Uhlenbeck (OU) process as the true signal

$$du(t) = ((-\gamma + \mathrm{i}\omega)u(t) + f(t))dt + \sigma dW(t), \tag{26}$$

where γ is damping, ω is oscillation frequency, $f(t)$ is external forcing, and σ is the strength of the white noise forcing. However, unlike the classical OU-process, which has constant damping, we consider the OU-process with time dependent damping $\gamma(t)$. In particular, we choose the damping that is modeled by a two-state Markov chain. This way, damping takes one of the two constant values, positive and negative. The positive value corresponds to stable dynamics and negative damping corresponds to unstable dynamics. We choose the time averaged damping to be positive to ensure a statistically stable dynamics. This OU-process with two-state Markov damping coefficients is designed to mimic signals from "nature", such as nonlinear chaotic stochastic dynamical systems with stable and unstable regimes of behavior. A concrete example from atmosphere ocean science of this regime-like behavior is monitoring one Rossby wave amplitude of a baroclinic fluid as the mean state randomly changes between regimes of stability and baroclinic instability [21]. Next, we describe how the Markov switching model chooses the value of the damping at each time.

3.1. Two-state Markov switching model

Here, we give a brief review about the two-state continuous-time Markov process. For a much more extensive discussion of the finite-state Markov chains see [30]. Consider a stochastic process $X(t)$ that can only take one of the two values

$$S = \{s_{st}, s_{un}\},$$

which correspond to stable and unstable dynamics, for example. Suppose, the system is in the stable state s_{st} at the initial time t_0. We define

$$T_{st} = \inf\{t : X(t) = s_{un}, t > t_0\}$$

to be the time during which the system stays in this stable state before it switches to the unstable one. We can use the definition of ν as a rate of leaving state s_{st} to find that

$$P(T_{st} \leqslant \Delta t) = \nu\Delta t + o(\Delta t).$$

This implies an exponential distribution of T_{st} with parameter ν

$$P(T_{st} < \tau) = 1 - e^{-\nu\tau},$$

where $\tau = t - t_0$. Similarly, the time T_{un} that the system spends in the unstable regime is an exponential random variable with the distribution

$$P(T_{un} < \tau) = 1 - e^{-\mu\tau}.$$

Let us now use the two-state Markov chain defined here in order to model the switching of damping $\gamma(t)$ of the signal $u(t)$ governed by Eq. (26). Suppose that damping $\gamma(t)$ switches between the values $d^+ = 2.27$ (stable phase) and $d^- = -0.04$ (unstable phase). Moreover, we set $\nu = 0.1$ and $\mu = 0.2$ such that the system should spend on average 10 time units in the stable regime and five time units in the unstable regime. The average damping of the system becomes

$$\bar{d} = \frac{\nu d^- + \mu d^+}{\nu + \mu} = 1.5. \tag{27}$$

3.2. Generating the true signal

Now, we can outline the procedure for how we generate the true signal. First of all, we generate a time series for the evolution of the damping $\gamma(t)$ using the exponential distribution of switching times as discussed in the previous section. Since

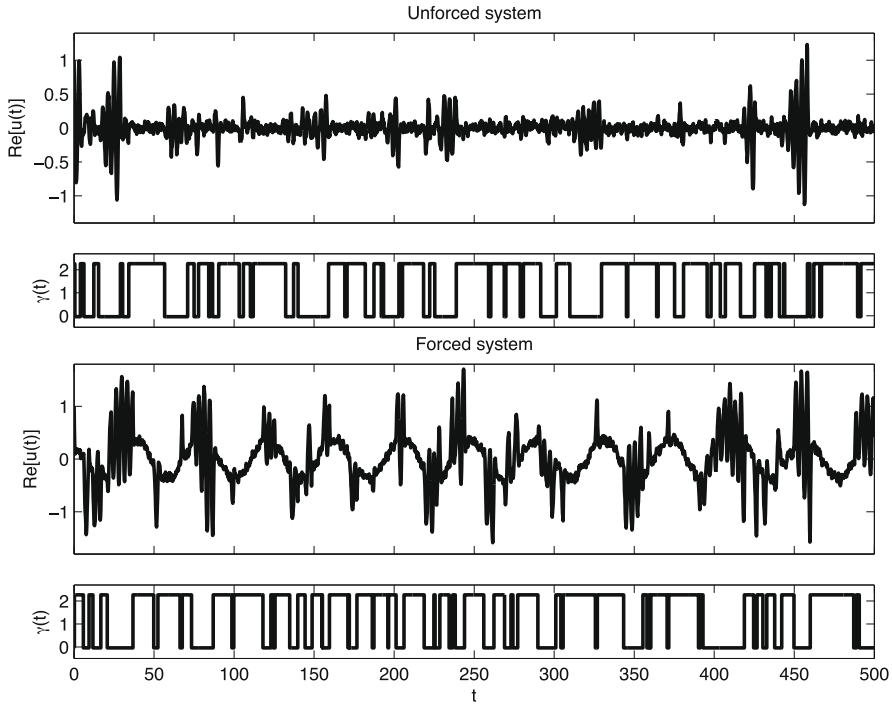

Fig. 2. Unforced (first panel) and forced (third panel) versions of the true trajectory (Re[$u(t)$] shown) with switching damping, $\gamma(t)$, (second and forth panels for the unforced and forced case, correspondingly).

the damping in the model is piecewise constant, the solution $u(t)$ can be exactly computed on each interval $[t_0, t_1]$, where $\gamma(t) = \text{const}$. For example, in the stable regime with $\gamma(t) = d^+$ we obtain

$$u(t_1) = u(t_0)e^{(-d^+ + i\omega)(t_1 - t_0)} + \int_{t_0}^{t_1} f(s)e^{(-d^+ + i\omega)(t_1 - s)}ds + \sigma \int_{t_0}^{t_1} e^{(-d^+ + i\omega)(t_1 - s)}dW(s).$$

Then if on the next time interval $[t_1, t_2]$, the system is in the unstable phase with $\gamma(t) = d^-$, we find the following solution

$$u(t_2) = u(t_1)e^{(-d^- + i\omega)(t_2 - t_1)} + \int_{t_1}^{t_2} f(s)e^{(-d^- + i\omega)(t_2 - s)}ds + \sigma \int_{t_1}^{t_2} e^{(-d^- + i\omega)(t_2 - s)}dW(s).$$

Now, before we show a representative generated trajectory, we discuss typical parameters for (5) which we use in this paper. We take $\bar{d} = 1.5,\ \omega = 1.78,\ \sigma = 0.1549$. We also introduce the typical energy of $u(t)$ to be the long time variance $E = \sigma^2/2\bar{d}$. These values correspond to the typical damping, oscillation and energy spectrum of an intermediate (in our example, we choose the 5th) mode of a barotropic Rossby waves that exhibits intermittent baroclinic instability [21] with the average 3 day decorrelation time.

In Fig. 2, we demonstrate the sample trajectories $u(t)$ given by Eq. (26) and the corresponding evolution of the damping $\gamma(t)$. The first and second panels of Fig. 2 correspond to the unforced case with $f(t) = 0$; the third and fourth panels of Fig. 2 correspond to the forced case with $f(t)$ given by Eq. (6) with $A_f = 1$ and $\omega_f = 0.15$. Note that in both forced and unforced cases, the regions of instability with $\gamma(t) = d^-$ are reflected by the significant growth of the signal $u(t)$ around its mean state. However the mean states are different: in the unforced case the mean state is zero and in the forced case the mean background is induced by the oscillatory external forcing $f(t)$. The trajectories shown in Fig. 2 will be used below for testing filtering skill of the combined, multiplicative and additive models, discussed in Section 2.

4. Improving filtering with model errors through stochastic parameter estimation

We begin this section by discussing the classical Kalman filter with the perfectly specified model. As we discussed in Section 1, unfortunately, the true dynamics are often unknown and hence model errors are unavoidable. The simplest commonly used approach, the Mean Stochastic Model (MSM), is discussed and used as a benchmark. Subsequently, we introduce the Stochastic Parameterization Extended Kalman Filter (SPEKF) as a new filtering approach that includes stochastic parameter estimation to improve the filtering skill in the presence of model errors. In Sections 4.2–4.4, we numerically check the filter performance for the unforced case, the forced case, and the case with incorrect forcing specification, consecutively. We then conclude this section with a brief summary of the filter performance.

4.1. Suite of filters

The classical Kalman filter [29,12] is an optimal two-step predictor and corrector method that includes observations at discrete time to adjust the prediction when the filter and observation models are linear and Gaussian. For equidistance discrete time setting, $t_{m+1} = t_m + \Delta t$, the Kalman filtering problem can be written as follows

$$u_{m+1} = F_{m+1}u_m + f_{m+1} + \sigma_{m+1}, \tag{28}$$

$$v_{m+1} = Gu_{m+1} + \sigma^o_{m+1}, \tag{29}$$

where in Eq. (28), the true signal $u_m \in \mathbb{C}^N$ is the quantity of interest at time $t_m, F_m \in \mathbb{C}^{N\times N}$ is the discrete linear deterministic operator that maps $u(t)$ forward in time, $f_m \in \mathbb{C}^N$ is an external forcing at time t_m, the N-dimensional complex valued noise $\sigma_m = (\sigma_{m,1} + \mathrm{i}\sigma_{m,2})/\sqrt{2}$ is defined with Gaussian white noise components $\{\sigma_{m,i} \in \mathbb{R}^N, i = 1,2\}$ with mean zero and variance $r_m \in \mathbb{C}^{N\times N}$. Observation $v_m \in \mathbb{C}^M$ is modeled as a transformation of the true signal u_m via linear operator $G \in \mathbb{C}^{M\times N}$ plus a complex Gaussian noise $\sigma^o_m = (\sigma^o_{m,1} + \mathrm{i}\sigma^o_{m,2})/\sqrt{2} \in \mathbb{C}^M$, where each component $\{\sigma^o_{m,i} \in \mathbb{R}^M, i = 1,2\}$ has zero mean and variance $r^o \in \mathbb{C}^{M\times M}$.

4.1.1. Perfectly specified model

The basic Kalman filter solution to (28) and (29) produces an estimate of the mean and covariance of u_{m+1} prior and posterior to knowing observation v_{m+1} [29,12–14]. The prior mean state and covariance are denoted by $\bar{u}_{m+1|m}$ and $r_{m+1|m}$, consecutively, while the posterior mean state and covariance are denoted by $\bar{u}_{m+1|m+1}$ and $r_{m+1|m+1}$, consecutively. These statistics are dynamically updated as follow:

Prior update:

$$\bar{u}_{m+1|m} = \widetilde{F}_{m+1}\bar{u}_{m|m} + \tilde{f}_{m+1}, \tag{30}$$

$$r_{m+1|m} = \widetilde{F}_{m+1}r_{m|m}\widetilde{F}^*_{m+1} + \tilde{r}_{m+1}. \tag{31}$$

Posterior update:

$$\bar{u}_{m+1|m+1} = \bar{u}_{m+1|m} + K_{m+1}(v_{m+1} - G\bar{u}_{m+1|m}), \tag{32}$$

$$r_{m+1|m+1} = (\mathcal{I} - K_{m+1}G)r_{m+1|m}, \tag{33}$$

$$K_{m+1} = r_{m+1|m}G^*(Gr_{m+1|m}G^* + r^o)^{-1}, \tag{34}$$

where the asterisk '*' in Eqs. (31) and (34) denotes the complex adjoint, $\widetilde{F}$ denotes the filter model deterministic operator, and $\tilde{r}$ denotes the filter model variance. The posterior mean update, $\bar{u}_{m+1|m+1}$, in (32) is simply a linear combination between the prior mean state, $\bar{u}_{m+1|m}$, and observation, v_{m+1}, weighted in accordance to the Kalman gain matrix $K_{m+1} \in \mathbb{C}^{N\times M}$. In the remainder of this paper, the signal we filter is a single complex value (see Section 3), therefore in the perfectly specified model setting $M = N = 1$ and the observation operator G is nothing but simply a scalar quantity; we choose $G = 1$. For scalar problems, the Kalman gain is bounded by $0 \leqslant K_m \leqslant 1$ and the filter weights fully toward the prior mean state (model) when $K_m = 0$ and fully toward the observation when $K_m = 1$ (see Eq. (32)).

In the perfectly specified model setting, the exact true dynamics as in (28) are used to propagate the mean and covariance forward in time. Given the true dynamics discussed in Section 3, we have

$$\widetilde{F}_{m+1} = F_{m+1} = \exp\left(-\int_{t_m}^{t_{m+1}} \gamma(s)ds + \mathrm{i}\omega\Delta t\right), \tag{35}$$

$$\tilde{r}_{m+1} = r_{m+1} = \frac{\sigma^2}{2\bar{d}}\left(1 - e^{-2\bar{d}\Delta t}\right), \tag{36}$$

$$\tilde{f}_{m+1} = f_{m+1}, \tag{37}$$

where $\Delta t = t_{m+1} - t_m$ denotes the observation time.

4.1.2. Mean Stochastic Model (MSM)

In reality, the true dynamics in Eq. (28) are unknown and what is available is long time average statistics of the true signal based on various measurements from past events, such as the equilibrium average decorrelation time $1/\bar{d}$ and the equilibrium variance $E = \sigma^2/2\bar{d}$ (in turbulence theory, this quantity is also called the equilibrium energy). The simplest commonly used filter model [24,25] is the Mean Stochastic Model (MSM), based on these equilibrium statistical quantities; MSM is

exactly the climatological stochastic model (CSM) in [24,25]. Specifically, the Mean Stochastic Model prior mean state and covariance are updated with the following deterministic dynamical operator:

$$\widetilde{F}_{m+1} = \exp\{(-\bar{d} + \mathrm{i}\omega)\Delta t\}, \tag{38}$$

where $\bar{d}$ is the average damping in (27) and use exactly the same $\tilde{r}_{m+1}$ and $\tilde{f}_{m+1}$ as in the perfectly specified model. We shall see in Sections 4.2–4.4 that this standard approach has large model error in general, especially when many transitions between stable and unstable regimes occur.

4.1.3. Stochastic Parameterization Extended Kalman Filter (SPEKF)

The classical approach for online estimation of model errors in the context of filtering (or data assimilation) is to append the parameters that represent model error (additive bias correction, $b(t)$) to the state vector $u(t) \in \mathbb{C}^N$ and filter the augmented system $(u(t), b(t)) \in \mathbb{C}^{2N}$ with the Kalman filter formula in (32) and (33) such that the observation operators $G \in \mathbb{C}^{M\times 2N}$ (see [7]). In many applications [5,4,3,6–9], this approach has been advocated with various assumptions on the dynamics of $b(t)$; the two most popular choices are with constant dynamics for $b(t)$ and random white noise. Our approach is motivated by this classical bias correction augmentation, however we consider Ornstein–Uhlenbeck processes on the additive bias correction term $b(t)$ and a multiplicative bias correction term $\gamma(t)$; the latter yields a nonlinear model as discussed in Section 2.

4.1.3.1. The combined model (SPEKF-C). The combined (multiplicative and additive) augmented system (5) with its observations is given as follows:

$$du(t) = [(-\gamma(t) + \omega\mathrm{i})u(t) + b(t) + f(t)]dt + \sigma dW_u(t), \tag{39}$$

$$db(t) = (-\gamma_b + \omega_b\mathrm{i})(b(t) - \hat{b})dt + \sigma_b dW_b(t), \tag{40}$$

$$d\gamma(t) = -d_\gamma(\gamma(t) - \hat{\gamma})dt + \sigma_\gamma dW_\gamma(t), \tag{41}$$

$$\begin{pmatrix} \mathrm{Re}(v_m) \\ \mathrm{Im}(v_m) \end{pmatrix} = G\begin{pmatrix} \mathrm{Re}[u_m] \\ \mathrm{Im}[u_m] \\ \mathrm{Re}[b_m] \\ \mathrm{Im}[b_m] \\ \gamma_m \end{pmatrix} + \begin{pmatrix} \sigma^o_{m,1} \\ \sigma^o_{m,2} \end{pmatrix}, \tag{42}$$

with the observation operator

$$G = \begin{pmatrix} 1 & 0 & 0 & 0 & 0 \\ 0 & 1 & 0 & 0 & 0 \end{pmatrix}. \tag{43}$$

Here $\{\sigma^o_{m,i}, i = 1, 2\}$ are independent Gaussian noises with mean zero and variance $r^o/2$. Eqs. (39)–(42) are solved at every discrete time t_m (when an observation is available), where $t_{m+1} = t_m + \Delta t$. The real observation model in Eq. (42) is very important in the filtering because, unlike in the perfectly specified model or MSM where cross covariances between the real and imaginary components are zero, there are significant cross covariances between the evolving components and parameters of the system, as shown in Section 2.4 and the Appendix.

Notice that there are five additional stochastic parameters $\{\gamma_b, \omega_b, \sigma_b, d_\gamma, \sigma_\gamma\}$ in this stochastic parameterization strategy for estimating two bias correction terms $b(t)$ and $\gamma(t)$ in Eqs. (40) and (41), which may seem to be inefficient. However, as we will find out below, this model filters the system effectively for a broad range of these five parameters. It is worth pointing out that we are not interested in finding optimal parameters for filter performance but robust parameter regimes with significantly improved filter skill for practical generalizations especially when higher dimensional systems are considered.

As discussed in Section 3, we typically observe only $u(t)$ in nature and therefore the observation operator is given as in (43). We refer to this filtering problem with both additive and multiplicative bias corrections in Eqs. (39)–(42) as the "Stochastic Parameterization Extended Kalman Filter-Combined model" (SPEKF-C) since the classical Extended Kalman Filter (EKF) linearizes the nonlinear system [13,14], whereas SPEKF uses the exact statistics to update the mean and covariances for $u(t), b(t), \gamma(t)$ between observation times, as derived in Section 2 and the Appendix. The formulas listed there show exponential growth of the mean and covariance in the exact statistics in time which can introduce large errors in using standard EKF for the augmented system.

4.1.3.2. The additive model (SPEKF-A). The simplest approach is to augment only the additive bias correction term $b(t)$ and set the damping term $\gamma(t)$ in (39) to be $\bar{d}$. In particular, we consider the following additive augmented system (7)

$$du(t) = [(-\bar{d} + \omega\mathrm{i})u(t) + b(t) + f(t)]dt + \sigma dW_u(t), \tag{44}$$

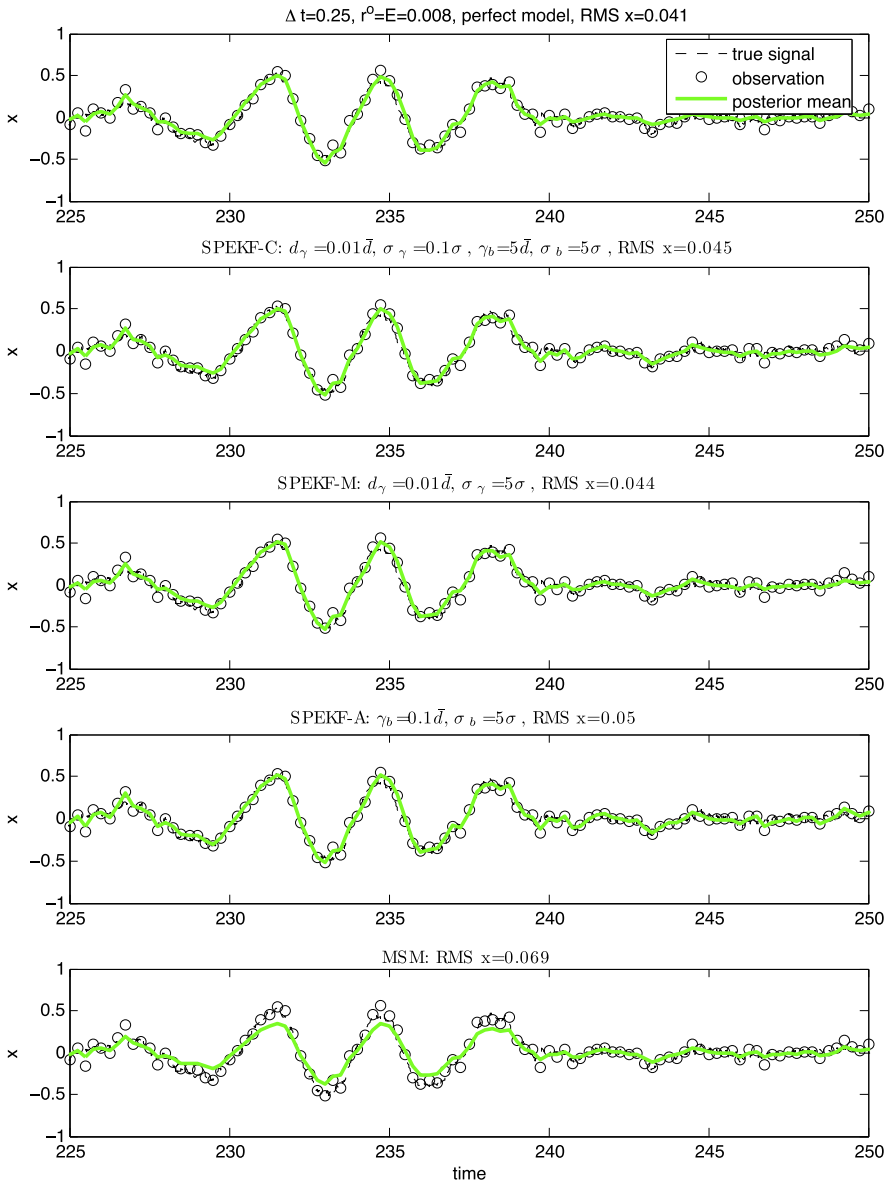

Fig. 3. Unforced case: posterior mean state $x(t) = \mathrm{Re}[u(t)]$ (thick solid line) as a function of time for simulations with $\Delta t = 0.25$, $r^o = E$ and stochastic parameters $\{\gamma_b = 0.1\bar{d}, \omega_b = \omega, \sigma_b = 5\sigma, d_\gamma = 0.01\bar{d}, \sigma_\gamma = 5\sigma\}$, compared with the true signals (dashes), and observations (circle).

$$db(t) = (-\gamma_b + \omega_b \mathrm{i})(b(t) - \hat{b})dt + \sigma_b dW_b(t), \tag{45}$$

$$\begin{pmatrix} \mathrm{Re}(v_m) \\ \mathrm{Im}(v_m) \end{pmatrix} = G \begin{pmatrix} \mathrm{Re}[u_m] \\ \mathrm{Im}[u_m] \\ \mathrm{Re}[b_m] \\ \mathrm{Im}[b_m] \end{pmatrix} + \begin{pmatrix} \sigma^o_{m,1} \\ \sigma^o_{m,2} \end{pmatrix}, \tag{46}$$

where

$$G = \begin{pmatrix} 1 & 0 & 0 & 0 \\ 0 & 1 & 0 & 0 \end{pmatrix}.$$

Note that as we mentioned earlier, in many applications the dynamics in (45) is often chosen to be $db(t) = 0$, $db(t) = \text{const.}$, or $db(t) = \sigma_b dW_b(t)$ [6,5,4,3].

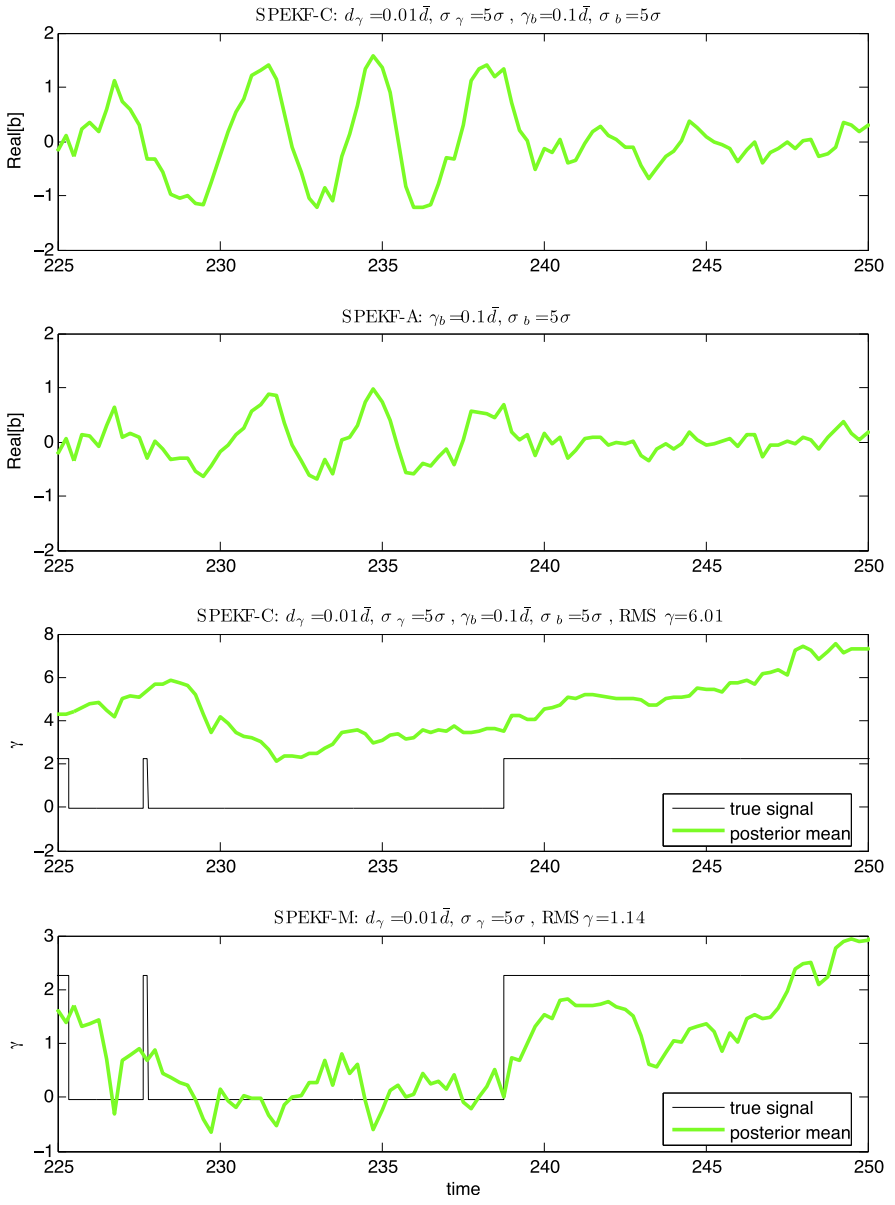

Fig. 4. Unforced case: posterior mean bias correction terms, Re$[b(t)]$ and $\gamma(t)$, as functions of time of the corresponding simulations in Fig. 3.

4.1.3.3. The multiplicative model (SPEKF-M). We also consider a simplified version of SPEKF with only the multiplicative bias correction term $\gamma(t)$. Formally, the filter problem can be written as follows:

$$du(t) = [(-\gamma(t) + \omega \mathrm{i})u(t) + f(t)]dt + \sigma dW_u(t), \tag{47}$$

$$d\gamma(t) = -d_\gamma(\gamma(t) - \hat{\gamma})dt + \sigma_\gamma dW_\gamma(t), \tag{48}$$

$$\begin{pmatrix} \mathrm{Re}(v_m) \\ \mathrm{Im}(v_m) \end{pmatrix} = G \begin{pmatrix} \mathrm{Re}[u_m] \\ \mathrm{Im}[u_m] \\ \gamma_m \end{pmatrix} + \begin{pmatrix} \sigma^o_{m,1} \\ \sigma^o_{m,2} \end{pmatrix}, \tag{49}$$

where

$$G = \begin{pmatrix} 1 & 0 & 0 \\ 0 & 1 & 0 \end{pmatrix}.$$

To be consistent, we called this approach SPEKF-M, where 'M' denotes multiplicative model.

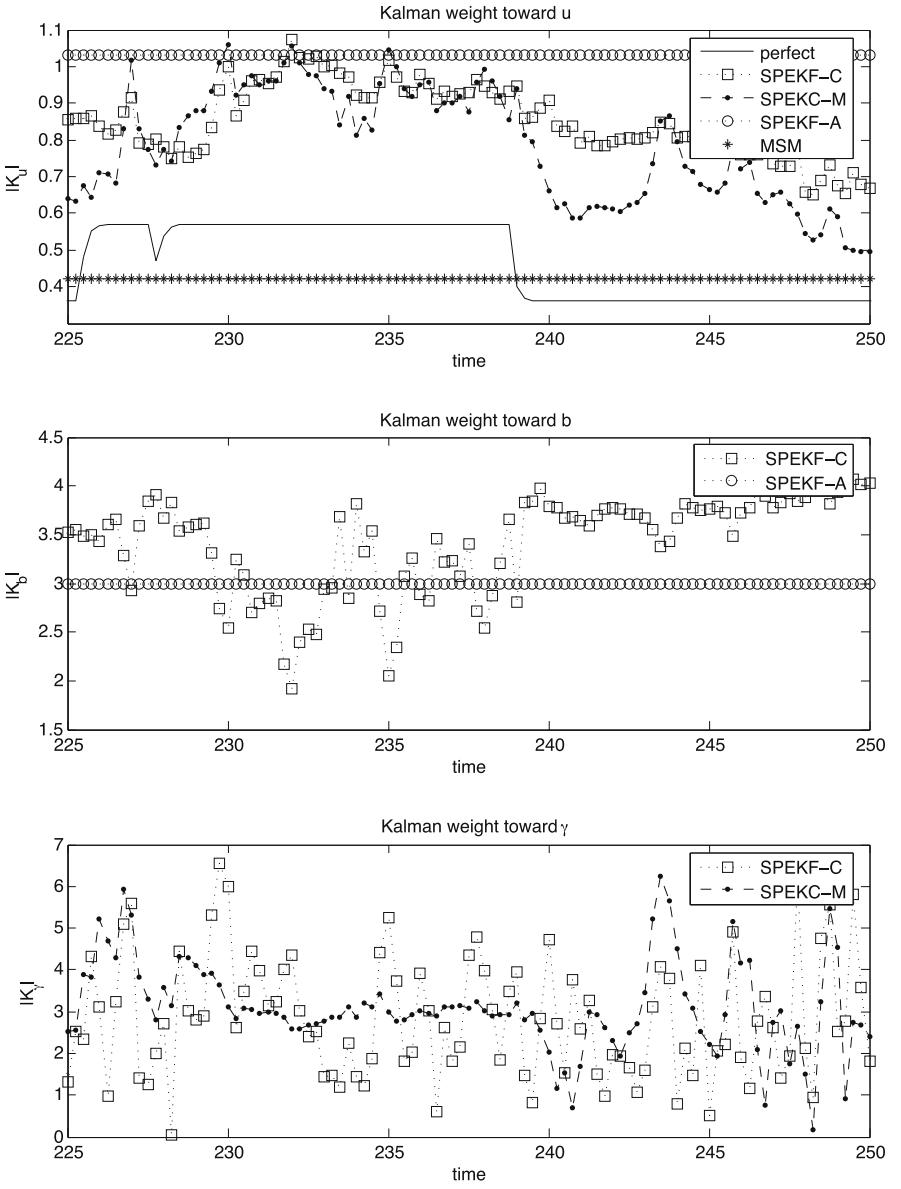

Fig. 5. Unforced case: Kalman weights toward $u(t)$, $b(t)$, and $\gamma(t)$ as functions of time of the corresponding simulations in Fig. 3.

4.2. Unforced case

In this section, we consider filter performance for the unforced case, $f(t) = 0$. We set $\hat{b} = 0$ since the additive bias is supposed to be perturbations around 0 and $\hat{\gamma} = \bar{d}$ since $\bar{d} = 1.5$ (see Section 3.2) is the average equilibrium damping strength. In each numerical simulation, we run the filter for $n = 2000$ assimilation cycles and we quantify the performance by computing the Root-Mean-Square (RMS) difference between the true signal, u_m, and the posterior mean state, $\bar{u}_{m|m}$,

$$\mathcal{E} = \sqrt{\frac{1}{n}\sum_{m=1}^{n} |\bar{u}_{m|m} - u_m|^2}.$$

First, we show the filter performance for $\Delta t = 0.25$ (shorter than the equilibrium average decorrelation time $1/\bar{d} \approx 0.66$) and observation noise variance $r^o = E = 0.008$, where $E = \sigma^2/2\bar{d}$ is the equilibrium variance of the true signal. In Fig. 3, we show

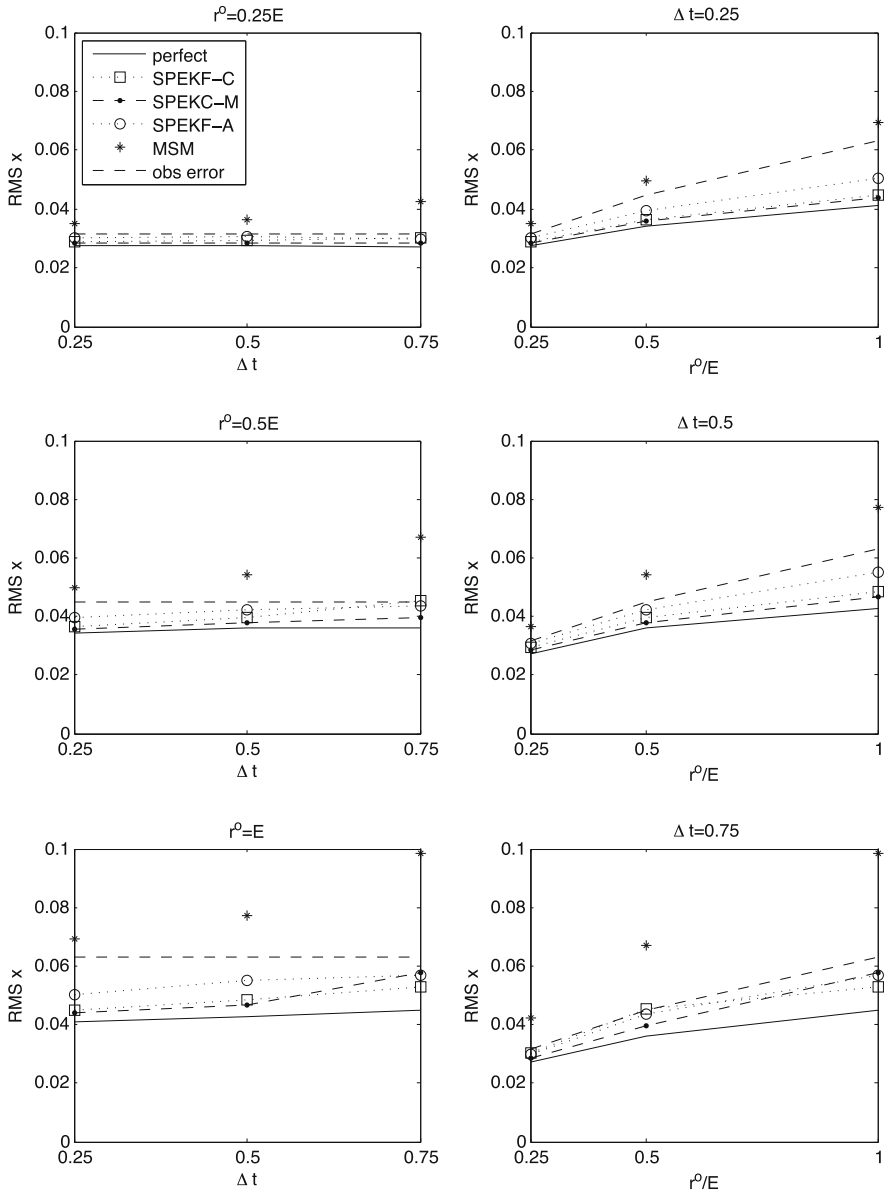

Fig. 6. Unforced case: average RMS errors as functions of observation times (first column) for fixed $r^o = 0.25E,\ 0.5E$, and E and as functions of relative observation noise variances, r^o/E, (second column) for fixed observation times $\Delta t = 0.25,\ 0.5,\ 0.75$.

trajectories of $x(t) = \mathrm{Re}[u(t)]$ for $\{\bar{d} = 1.5, \omega = 1.78, \sigma = 0.1549\}$ (as in Section 3.2) with stochastic parameters $\{\gamma_b = 0.1\bar{d}, \omega_b = \omega, \sigma_b = 5\sigma, d_\gamma = 0.01\bar{d}, \sigma_\gamma = 5\sigma\}$ for SPEKF-C, $\{d_\gamma = 0.01\bar{d}, \sigma_\gamma = 5\sigma\}$ for SPEKF-M, $\{\gamma_b = 0.1\bar{d}, \omega_b = \omega, \sigma_b = 5\sigma\}$ for SPEKF-A, and compare their skill with the perfectly specified model and MSM. These stochastic parameter sets are obtained empirically and their robustness will be discussed later in more detail. We find that all three SPEKFs are almost as skillful as the perfectly specified model; the RMS errors of the perfectly specified model is 0.04 and SPEKFs are roughly 0.045–0.05, which is 25% less than simply trusting the observations with error $\sqrt{r^o/2} \approx 0.06$. The MSM, on the other hand, misses some of the peaks in the unstable regime (see Fig. 3) and its RMS error, 0.07, is larger than the observation error.

In Fig. 4, we plot the corresponding bias correction terms, $\mathrm{Re}[b(t)]$ and $\gamma(t)$, for the same simulations. We find that the additive bias correction term, $b(t)$, in SPEKF-C and SPEKF-A with damping time scale $1/\gamma_b \approx 6.6$, learns the model errors based on the given observations; it provides a significant bias correction whenever the system is unstable and small bias correction in the stable regime. In the last two panels of Fig. 4, we notice a significant difference between SPEKF-C and SPEKF-M in tracking $\gamma(t)$ although the filtering skill in $u(t)$ is nearly similar. The simulations suggest that

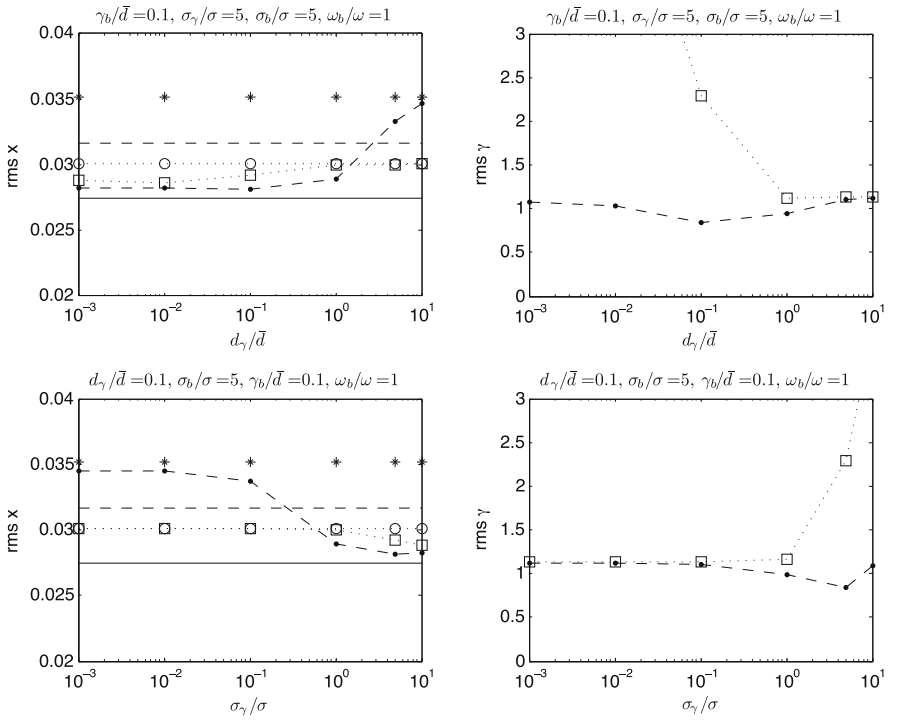

Fig. 7. Unforced case: average RMS errors of $x(t) = \mathrm{Re}[u(t)]$ (first columns) and $\gamma(t)$ (second column) as functions of multiplicative stochastic parameters $\{d_\gamma, \sigma_\gamma\}$ for simulations with observation time $\Delta t = 0.25$ and observation noise variance $r^o = 0.25E$. In each panel, we depict the RMS errors for the perfectly specified model (solid), SPEKF-C (square), SPEKF-M (dash-dotted), SPEKF-A (circle), MSM (asterisk), and observation error (dashes).

SPEKF-C does not need an accurate prediction of $\gamma(t)$ for accurate prediction of $u(t)$ since $b(t)$ plays a significant role in correcting the bias while $\gamma(t)$ is only the tendency of bias correction. On the other hand, when additive bias correction term, $b(t)$, is absent as in SPEKF-M, more accurate prediction of $\gamma(t)$ is necessary for high filter skill in predicting $u(t)$.

Fig. 5 shows the corresponding amplitude of the Kalman gain matrix on variables $u(t), b(t)$, and $\gamma(t)$ for the simulations in Fig. 3. We define these amplitudes by

$$|K_u| = \sqrt{K_{1,1}^2 + K_{2,2}^2},$$

$$|K_b| = \sqrt{K_{3,1}^2 + K_{4,2}^2},$$

$$|K_\gamma| = \sqrt{K_{5,1}^2 + K_{5,2}^2},$$

for the fully combined model in which the Kalman gain matrix is $K \in \mathbb{R}^{5\times 2}$. For SPEKF-A, only $|K_u|$ and $|K_b|$ exist since $K \in \mathbb{R}^{4\times 2}$; for SPEKF-A, only $|K_u|$ and $|K_\gamma| = \sqrt{K_{3,1}^2 + K_{3,2}^2}$ exist since $K \in \mathbb{R}^{3\times 2}$. The numerical experiments suggest that the perfectly specified model, SPEKF-C, and SPEKF-M weigh more toward the observations (larger $|K_u|$) in the unstable regime and more toward the model in the stable regime (smaller $|K_u|$). The Kalman weight $|K_u|$ of SPEKF-A and MSM are constant since they both are linear filters. We are especially interested in the Kalman weights of the parameters $b(t), \gamma(t)$ which indicate how much information is transferred to these parameters from the observed signals. The variations in the Kalman weight toward $b(t)$ suggests substantial learning in both SPEKF-C and SPEKF-A. Here, $|K_b|$ for SPEKF-C weighs more toward observations in the stable regime and more toward the model in the unstable regime; this behavior is opposite to $|K_u|$. In this simulation, we find that the Kalman weights toward $\gamma, |K_\gamma|$ for SPEKF-C and SPEKF-M are on the same order, but later in the forced case (see Fig. 15), we will see that the Kalman weight $|K_\gamma|$ for SPEKF-C is mostly smaller than that for SPEKF-M, which confirms the importance of $b(t)$ compared with $\gamma(t)$.

In Fig. 6, we show the RMS errors for the same stochastic parameters as above for various observation times $\Delta t = 0.25, 0.5, 0.75$ and relative observation error variances $r^o/E = 0.25, 0.5, 1$. First, we note that MSM is consistently less

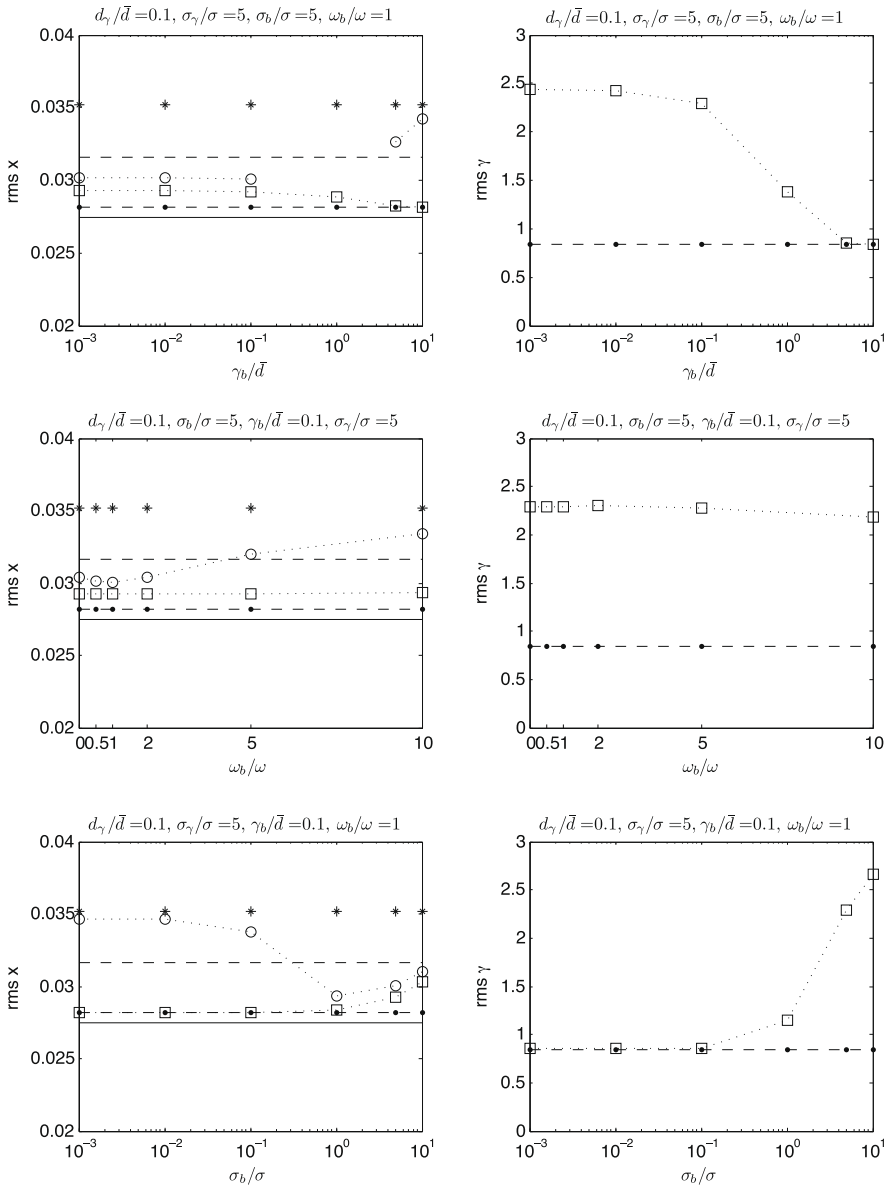

Fig. 8. Unforced case: average RMS errors of $x(t) = \mathrm{Re}[u(t)]$ (first columns) and $\gamma(t)$ (second column) as functions of additive stochastic parameters $\{\gamma_b, \omega_b, \sigma_b\}$ for simulations with observation time $\Delta t = 0.25$ and observation noise variance $r^o = 0.25E$. In each panel, we depict the RMS errors for the perfectly specified model (solid), SPEKF-C (square), SPEKF-M (dash-dotted), SPEKF-A (circle), MSM (asterisk), and observation error (dashes).

skillful than trusting the observations. We find that the skill of SPEKF-C, SPEKF-M, and SPEKF-A are similar and their skill is almost as good as the skill of the perfect model simulation in almost every regime. SPEKF-A is comparable to SPEKF-C when observation noise variance is small and it slightly deteriorates as the observation noise variance increases but still is much more skillful than MSM or even simply trusting the observations.

When observation noise variance, r^o, is large the filter tends to weigh more toward the model; the fact that the skill of all three SPEKFs are nearly as good as the skill of the perfectly specified model suggests that the additional bias corrections, b, γ, introduced in SPEKF, reduce the model errors significantly compared to MSM. When observation error is small, the skill disparity between SPEKFs and MSM becomes less transparent since the RMS error of the perfectly specified model is very similar to the observation error. We also find that the skill of SPEKFs decreases only slightly as the observation time increases even beyond the correlation time. In contrast, the filtering skill of MSM decreases significantly as a function of observation time since the model error is large. These large model errors are probably due to the increased stability transitions that can occur between infrequent observation times.

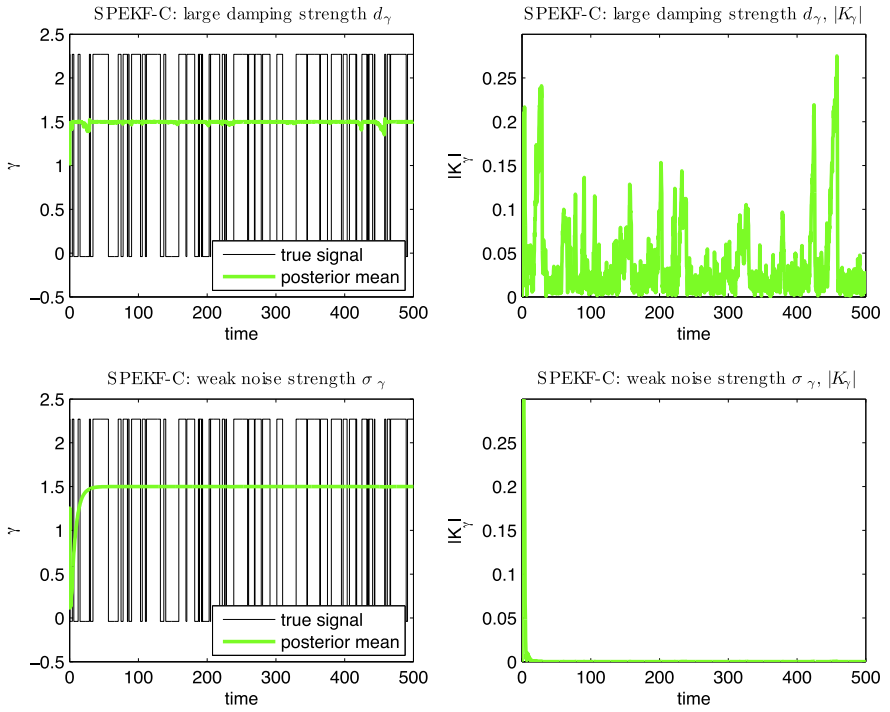

Fig. 9. Regime where SPEKF-M (or SPEKF-C with large damping $\gamma_b = 5\bar{d}$) fails: too strong damping, $d_\gamma = 10\bar{d}$, with $\sigma_\gamma = 5\sigma$ (first row) and too weak noise strength, $\sigma_\gamma = 0.1\sigma$, with fixed $d_\gamma = 0.1\bar{d}$ (second row). Both simulations are implemented with $\omega_b = \omega,\ \sigma_b = \sigma$. The first column shows the posterior mean of the multiplicative bias correction term, $\gamma(t)$, (in thick solid line) as well as the true damping (in thin solid line) as functions of time for strong damping and the second column shows the Kalman weight toward $\gamma(t)$.

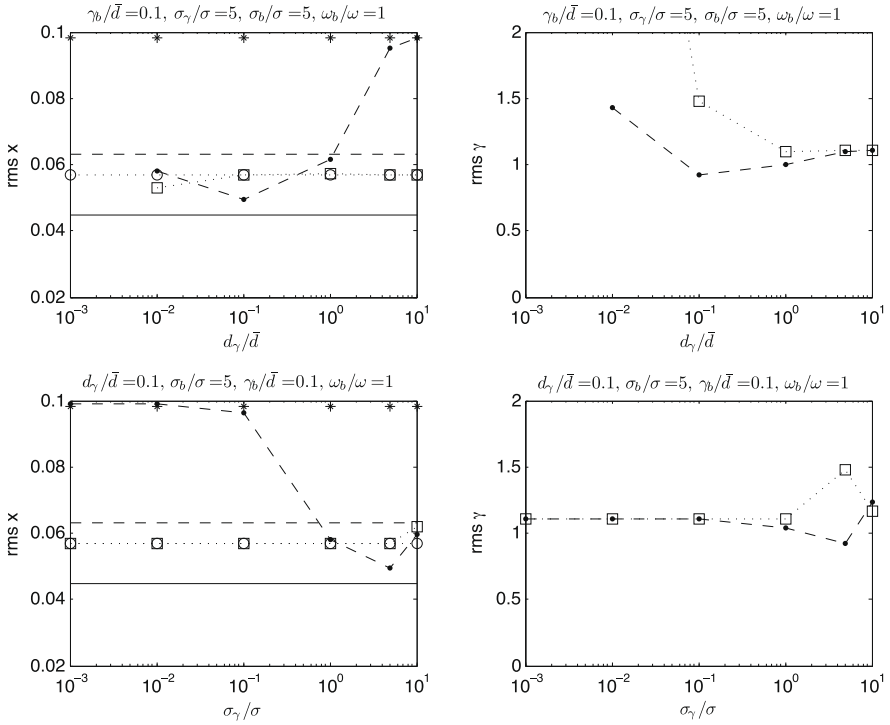

Fig. 10. Unforced case: average RMS errors of $x(t) = \mathrm{Re}[u(t)]$ (first columns) and $\gamma(t)$ (second column) as functions of multiplicative stochastic parameters $\{d_\gamma, \sigma_\gamma\}$ for simulations with observation time $\Delta t = 0.75$ and observation noise variance $r^o = E$. In each panel, we depict the RMS errors for the perfectly specified model (solid), SPEKF-C (square), SPEKF-M (dash-dotted), SPEKF-A (circle), MSM (asterisk), and observation error (dashes).

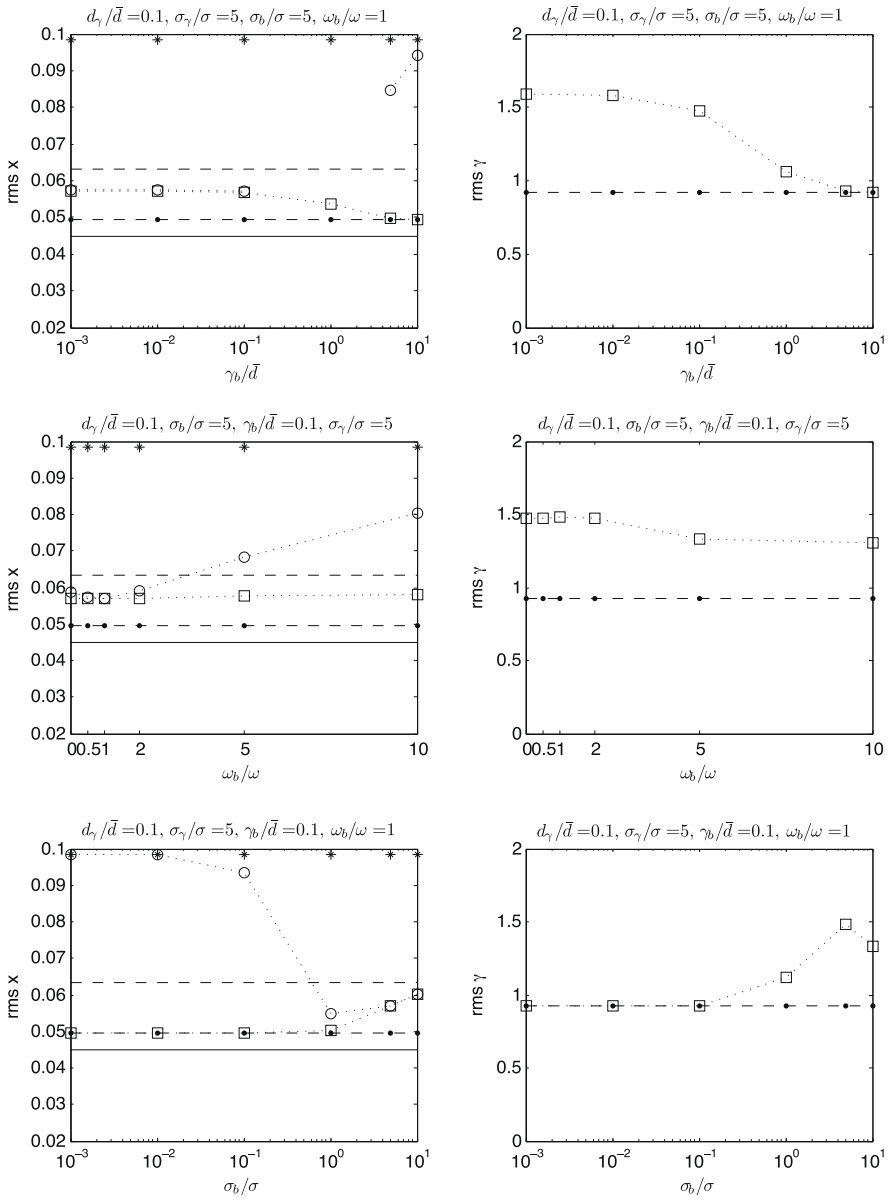

Fig. 11. Unforced case: average RMS errors of $x(t) = \mathrm{Re}[u(t)]$ (first columns) and $\gamma(t)$ (second column) as functions of additive stochastic parameters $\{\gamma_b, \omega_b, \sigma_b\}$ for simulations with observation time $\Delta t = 0.75$ and observation noise variance $r^o = E$. In each panel, we depict the RMS errors for the perfectly specified model (solid), SPEKF-C (square), SPEKF-M (dash-dotted), SPEKF-A (circle), MSM (asterisk), and observation error (dashes).

4.2.1. Robustness and sensitivity to stochastic parameters

Now we check the robustness and sensitivity of the filter toward variations of the following stochastic parameters $\{\gamma_b, \omega_b, \sigma_b, d_\gamma, \sigma_\gamma\}$. In Figs. 7 and 8, we show the RMS errors of $x(t) = \mathrm{Re}[u(t)]$ (first column) and $\gamma(t)$ (second column) for additive and multiplicative stochastic parameters for observation time $\Delta t = 0.25$ and observation noise variance $r^o = 0.25E$. In each row, we plot the RMS errors as functions of one of the stochastic parameters whereas the other four parameters are fixed such that SPEKF-C has small RMS error (they are documented on each panel). From Figs. 7 and 8, we find that the filtering skill of SPEKF-C is high for a wide range of parameter choices and is the most robust compared to SPEKF-M and SPEKF-A despite the existence of regimes where SPEKF-M beats SPEKF-C by an insignificant amount and regimes where SPEKF-A is comparable to SPEKF-C. The former situation is simply due to sampling error. Next, we discuss the parameter regimes with poor filter skill and analyze the failure there.

When the parameter γ_b is large, we find that the additive bias term, $b(t)$, adjusts quickly to $\hat{b} = 0$ and SPEKF-C behaves similarly to SPEKF-M. Hence, SPEKF-C performs as badly as SPEKF-M in this regime since the latter is sensitive to variation

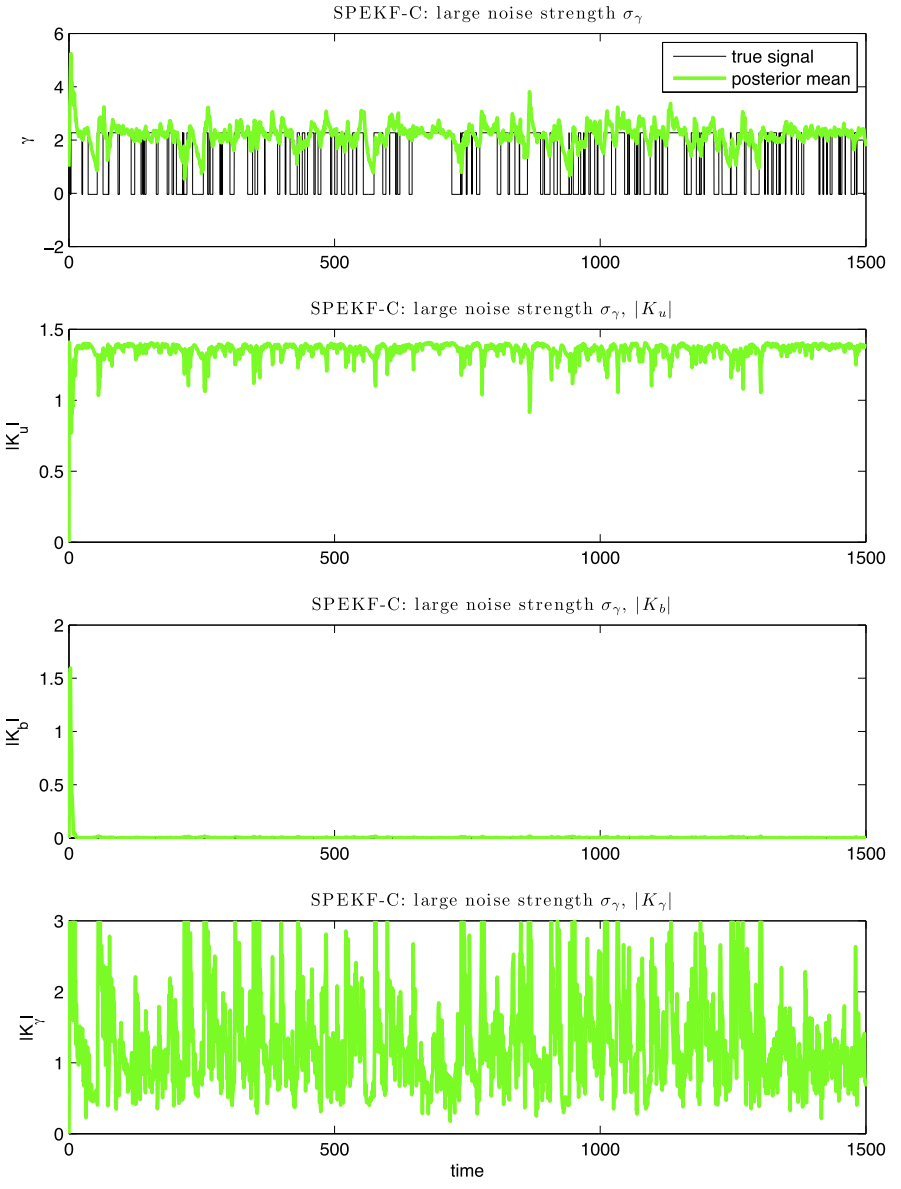

Fig. 12. Regime where SPEKF-M (or SPEKF-C with large damping $\gamma_b = 5\bar{d}$) fails: too strong noise, $\sigma_\gamma = 10\sigma$, with fixed $d_\gamma = 0.1\bar{d},\ \gamma_b = 0.1\bar{d},\ \omega_b = \omega$ and $\sigma_b = 0.1\sigma$. The first row shows the posterior mean of the multiplicative bias correction term, $\gamma(t)$, (in thick solid line) as well as the true damping (in thin solid line) as functions of time for strong damping and the last three rows show the Kalman weight toward $u(t),\ b(t)$, and $\gamma(t)$.

of parameters (again, see dash-dotted line in Fig. 7). The first scenario for SPEKF-M (and hence SPEKF-C with large damping γ_b) to fail is when the damping strength, d_γ, is too large. Here, the multiplicative bias correction term $\gamma(t)$ relaxes too quickly to the equilibrium average damping $\hat{\gamma} = \bar{d}$ and hence the multiplicative bias correction term $\gamma(t)$ becomes nothing more than a sampling of random perturbations around $\bar{d}$. Therefore, SPEKF-C (with large damping $\gamma_b = 5\bar{d}$) is not much more skillful than MSM, which has damping exactly $\gamma(t) = \bar{d}$ (see the first row of Fig. 9). In the same row, one can see that the Kalman weight toward $\gamma(t), |K_\gamma|$, is very small (compare it with the Kalman weight for high filtering skill in Fig. 5, there $|K_\gamma| = \mathcal{O}(1)$).

The second parameter regime with poor skill occurs when the noise strength σ_γ is too small; then, the multiplicative bias correction term $\gamma(t)$ is nothing but a decaying exponential solution and once it relaxes to $\bar{d}$ (see the second row in Fig. 9), again there is no more learning (as $|K_\gamma| \approx 0$) in SPEKF-C (again with large damping $\gamma_b = 5\bar{d}$) and its skill is as poor as the skill of MSM.

Earlier we found that the parameters of SPEKF-A can be tuned such that it is almost comparable to the perfectly specified model; however we find that its parameter regime is not as robust as that of SPEKF-C (again, see Fig. 8). In particular, numerical instability occurs when $\gamma_b = \bar{d}$ and $\omega_b = \omega$ (the second term in (11) in Section 2 is singular for $J(s,t) = 0$) and

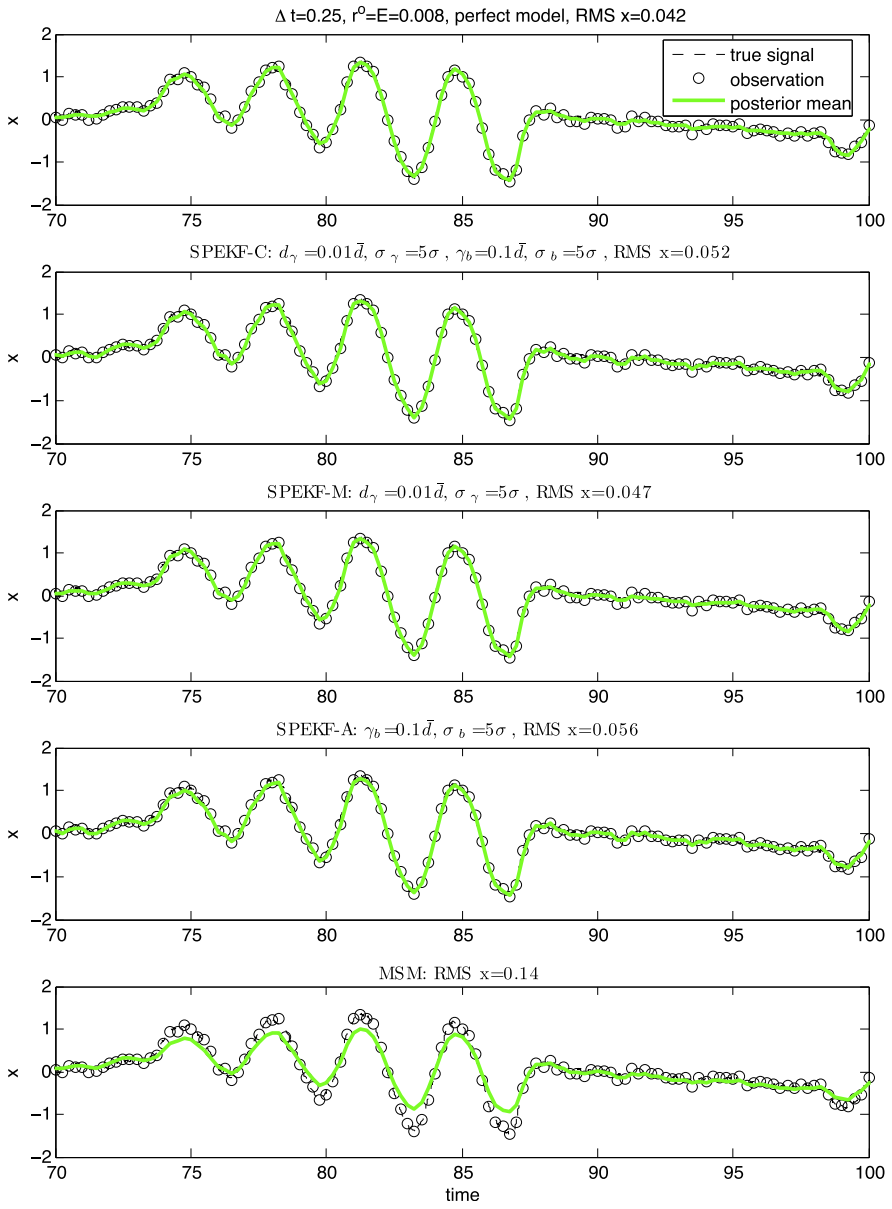

Fig. 13. Forced case: posterior mean state $x(t) = \mathrm{Re}[u(t)]$ (thick solid line) as a function of time for simulations with $\Delta t = 0.25$, $r^o = E$ and stochastic parameters $\{\gamma_b = 0.1\bar{d}, \omega_b = \omega, \sigma_b = 5\sigma, d_\gamma = 0.01\bar{d}, \sigma_\gamma = 5\sigma\}$, compared with the true signals (dashes), and observations (circle).

the filter diverges beyond machine infinity; also SPEKF-A is more sensitive toward variations of ω_b compared to SPEKF-C. Similar to the multiplicative correction term, $\gamma(t)$, when the damping strength is too large. $\gamma_b > \bar{d}$, the additive correction term, $b(t)$, is nothing but a tiny perturbation around zero; when σ_b is too small (less than σ), the additive correction term is an exponentially decaying solution.

The robustness above holds for a different observation time $\Delta t = 0.5$ (below the average equilibrium decorrelation time $1/\bar{d} \approx 0.66$) and various observation noise variances $r^o/E = 0.5, 1$ (not shown). Therefore, the results shown in Figs. 3–6 for parameter set $\{\gamma_b = 0.1\bar{d}, \omega_b = \omega, \sigma_b = 5\sigma, d_\gamma = 0.01\bar{d}, \sigma_\gamma = 5\sigma\}$ are robust.

Now we consider an observation time beyond the decorrelation time, $\Delta t = 0.75$. The RMS errors in Figs. 10 and 11 suggest that SPEKF-C is, again, the most robust strategy. Here, there are two more scenarios for SPEKF-C (with large damping γ_b) to fail in addition to the two scenarios discussed earlier. When the damping is too weak, $d_\gamma = 10^{-3}\bar{d}$, Eqs. 41, 48 are nearly identical to the Wiener process $d\gamma(t) = \sigma_\gamma dW_\gamma(t)$, with unbounded behavior for large times. When the multiplicative parameter noise $\sigma_\gamma = 10\sigma$ is too large (see Fig. 12), SPEKF-C tends to over estimate in both stable and unstable regimes. Specifically,

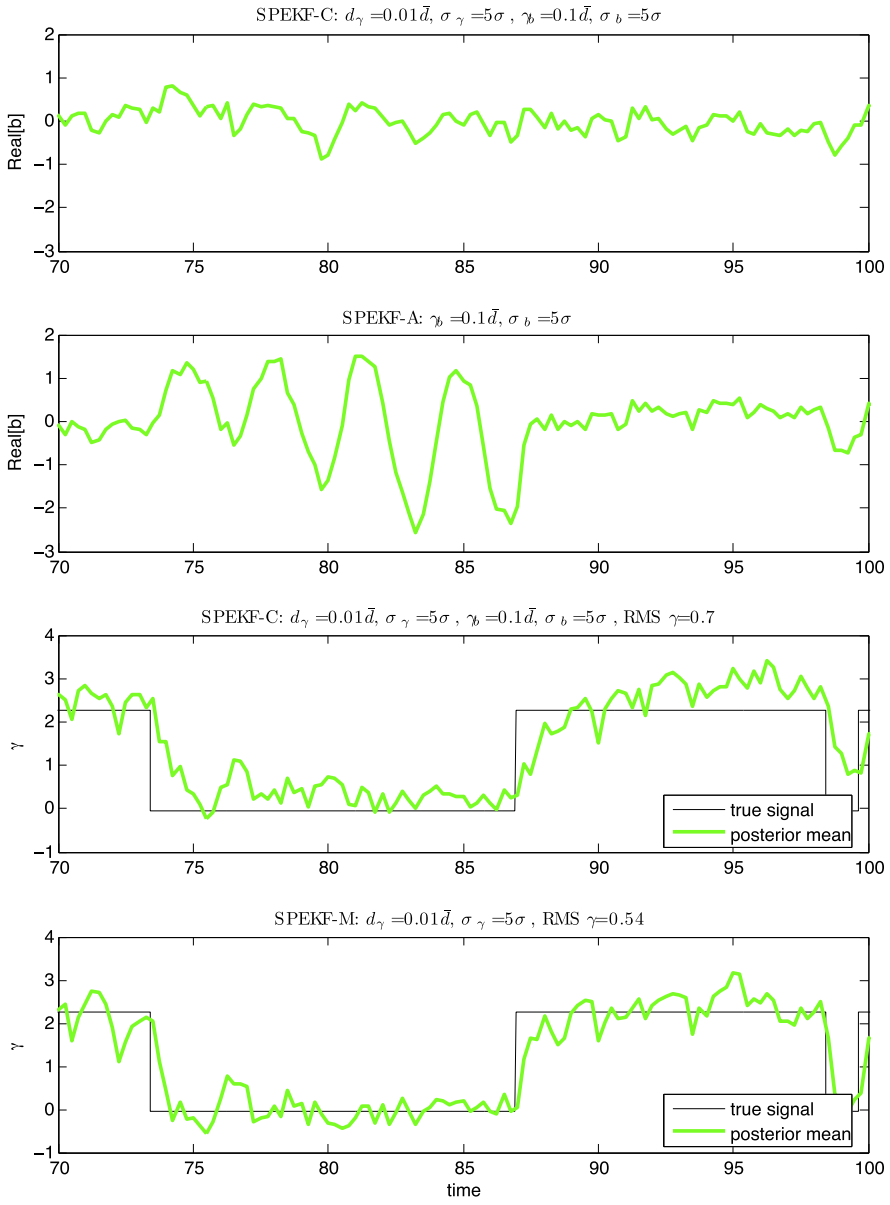

Fig. 14. Forced case: posterior mean bias correction terms, Re$[b(t)]$ and $\gamma(t)$, as functions of time of the corresponding simulations in Fig. 13.

there are almost no contributions from the additive bias correction term, $b(t)$, since $|K_b| \approx 0$. Simultaneously, the multiplicative terms are too noisy. Thus, the model errors are too large to avoid and hence the filtered solutions tend to weigh more toward observations.

4.3. Forced case

In this section, we consider filtering Eq. (26) with a smooth periodic forcing

$$f(t) = A_f e^{i\omega_f t},$$

where $A_f = 1,\ \omega_f = 0.15$ (same as in Section 3.2). As in the unforced case, discussed in Section 4.2, we set $\hat{b} = 0$ and $\hat{\gamma} = \bar{d}$. Observations are simulated by adding random Gaussian noises with mean zero and variance r^o to the true signal, as discussed in Section 2. As shown in Fig. 2, we anticipate that such forcing increases the model errors in MSM and yields a severe test for the stochastic parameter estimation strategies.

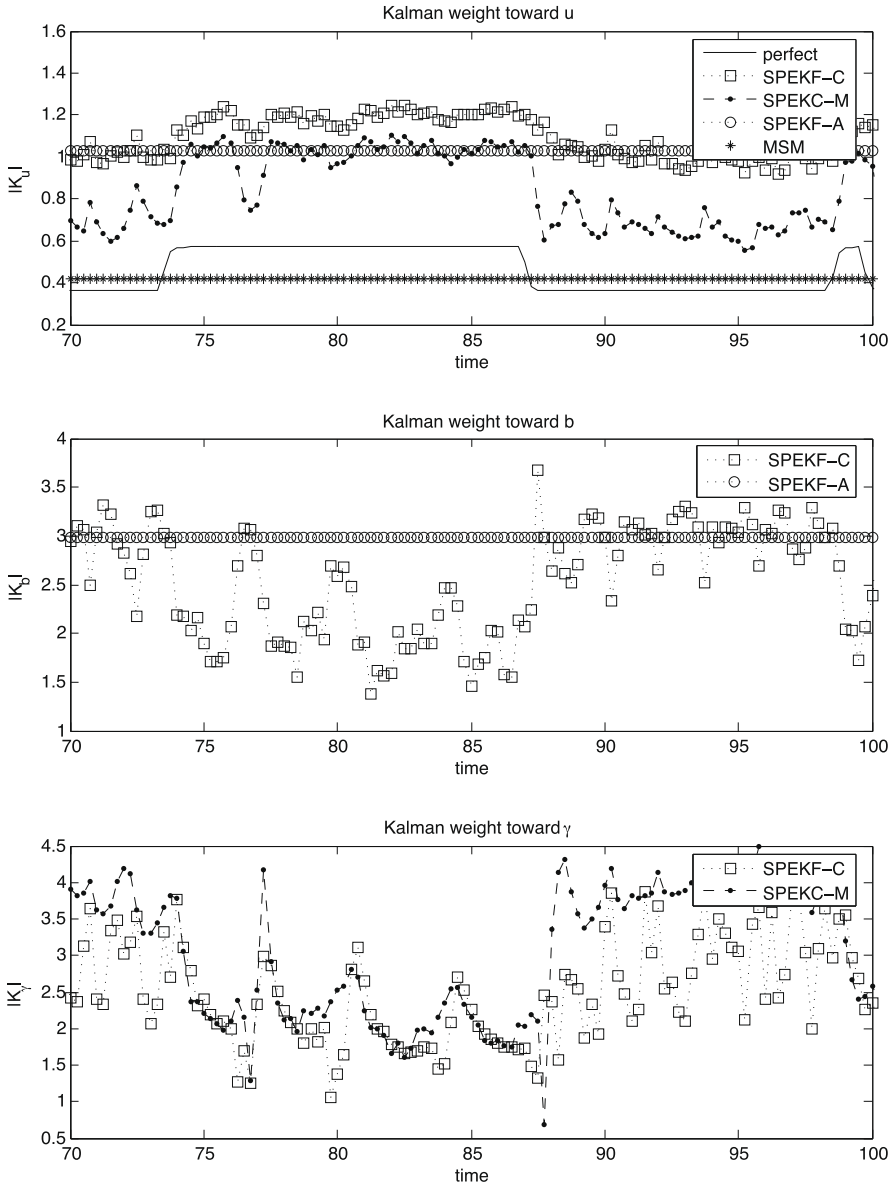

Fig. 15. Forced case: Kalman weights toward $u(t)$, $b(t)$, and $\gamma(t)$ as functions of time of the corresponding simulations in Fig. 13.

In Figs. 13–15, we show trajectories of the posterior mean states $u(t), b(t), \gamma(t)$, and the Kalman weights with parameter sets: $\{\gamma_b = 0.1\bar{d}, \omega_b = \omega, \sigma_b = 5\sigma, d_\gamma = 0.01\bar{d}, \sigma_\gamma = 5\sigma\}$ for SPEKF-C, $\{d_\gamma = 0.01\bar{d}, \sigma_\gamma = 5\sigma\}$ for SPEKF-M, and $\{\gamma_b = 0.1\bar{d}, \sigma_b = 5\sigma\}$ for SPEKF-A, for simulations with observation time $\Delta t = 0.25$ and observation noise variance $r^o = E = 0.008$. We find that SPEKFs are almost as skillful as the perfectly specified model and their RMS errors, 0.04–0.05, are smaller than the observation error, 0.06. On the other hand, the RMS error of MSM, 0.14, is more than twice as big as the observation error. As in the unforced case, this choice of parameter in SPEKF-C suggests a relatively significant contribution of additive bias correction (see $b(t) \approx \mathcal{O}(10^{-1})$ and $|K_b|$ fluctuates around 2.5 in Figs. 14 and 15), respectively. In Section 4.4, we shall see that the additive bias correction, $b(t)$, becomes even more significant when the forcing is specified incorrectly. Unlike the unforced case, here we find substantial skill in tracking $\gamma(t)$ with SPEKF-C (see Fig. 14) as well as SPEKF-M. This result suggests that the multiplicative bias correction term, $\gamma(t)$, in SPEKF-C becomes as important as the additive bias correction term, $b(t)$, when the forcing is nonzero.

We find that the performance skill for the forced case is qualitatively similar to the unforced case as the observation time and observation noise variances vary (see Fig. 16), except that the skill of the perfectly specified model is not very different compared to fully trusting the observations due to a larger signal to noise ratio. In Figs. 17 and 18, we also plot the RMS

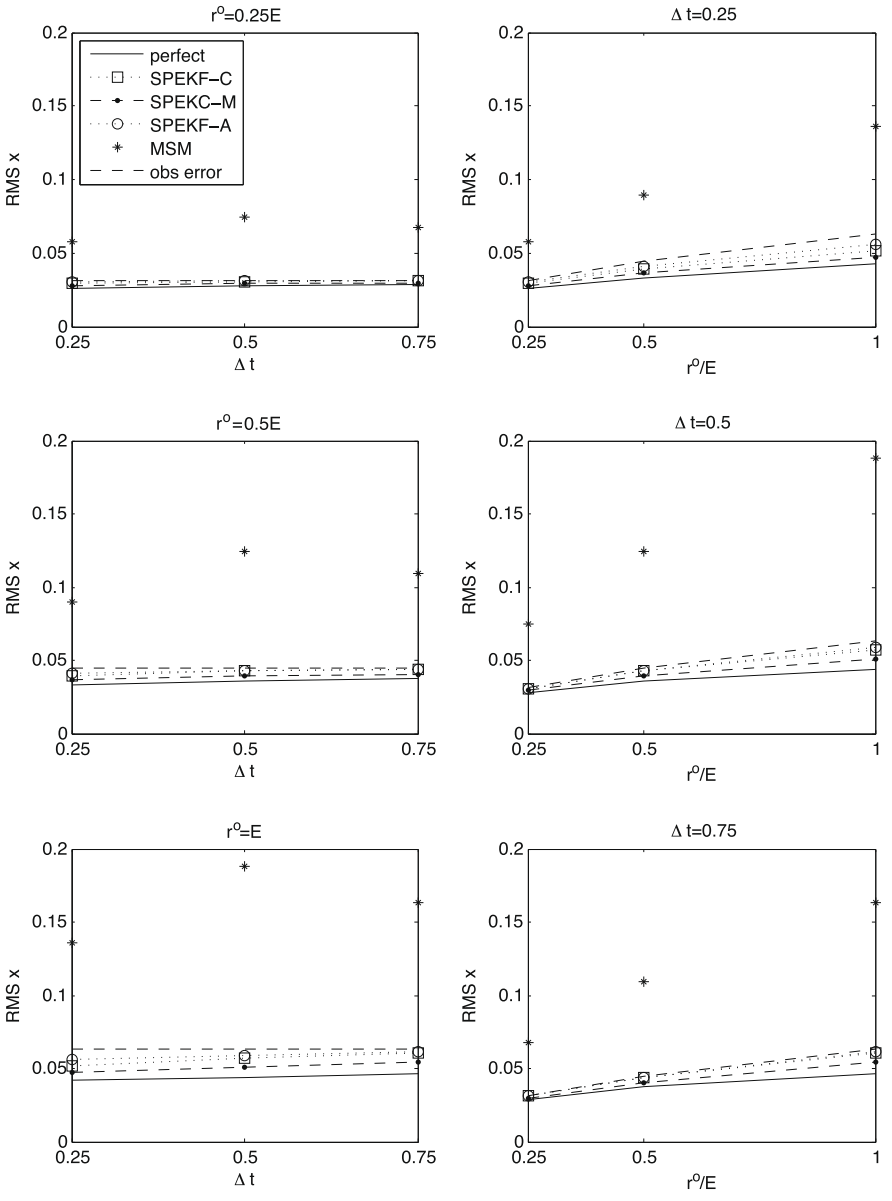

Fig. 16. Forced case: average RMS errors as functions of observation times (first column) for fixed $r^o = 0.25E,\ 0.5E$, and E and as functions of relative observation noise variances, r^o/E, (second column) for fixed observation times $\Delta t = 0.25,\ 0.5,\ 0.75$.

errors as functions of multiplicative and additive stochastic parameters for $\Delta t = 0.25$ and $r^o = 0.25E$. We find that the filter robustness and sensitivity toward stochastic parameters are similar to the unforced case as discussed earlier in Section 4.2.

4.4. Learning the forcing from the filtering

In this Section, we discuss the situation when the external forcing $f(t)$ is either partially known or unknown. If we regard the true signal as arising as a turbulent component of a more complex system, such a circumstance arises readily. In this situation, the additive bias correction term $b(t)$ is used as a learning tool for the external forcing. First, we consider the case when the external forcing is completely unknown. This is a severe test case; thus, we set $f(t) \equiv 0$ in Eq. (5) and apply the filters to recover a true signal that has the same forcing as in the previous section. In Fig. 19, we demonstrate the results of filtering using all three methods (SPEKF-C, SPEKF-M, and SPEKF-A) with the incorrectly prescribed external forcing. We note that the combined and additive models retain most of their skill in filtering $u(t)$ (RMS errors of SPEKF-C is 0.055 and

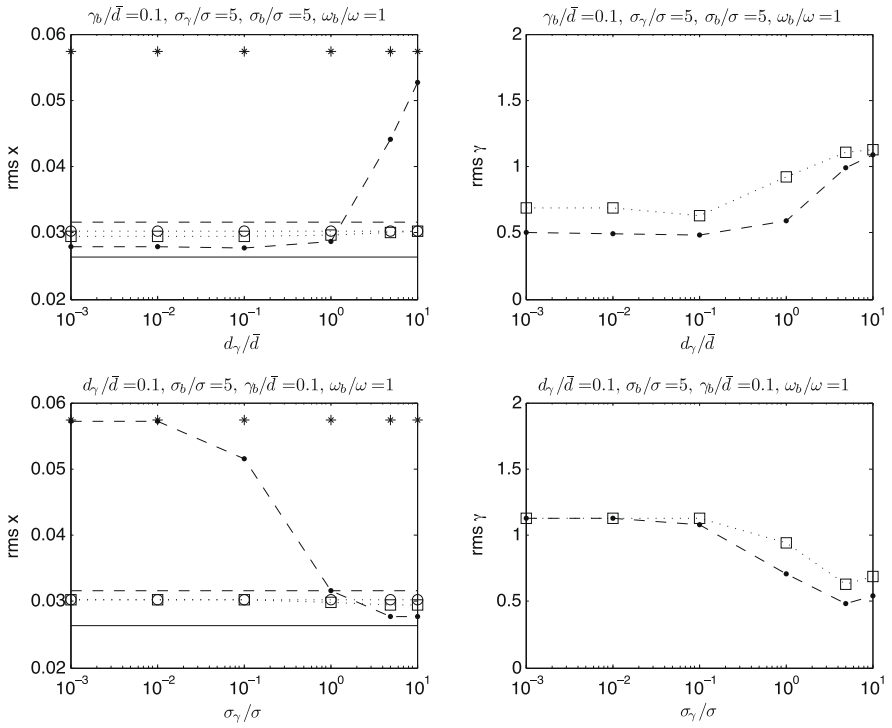

Fig. 17. Forced case: average RMS errors of $x(t) = \mathrm{Re}[u(t)]$ (first columns) and $\gamma(t)$ (second column) as functions of multiplicative stochastic parameters $\{d_\gamma,\ \sigma_\gamma\}$ for simulations with observation time $\Delta t = 0.25$ and observation noise variance $r^o = 0.25E$. In each panel, we depict the RMS errors for the perfectly specified model (solid), SPEKF-C (square), SPEKF-M (dash-dotted), SPEKF-A (circle), MSM (asterisk), and observation error (dashes).

of SPEKF-A is 0.059); on the other hand, the performance of the multiplicative model (with RMS error 0.111) became much worse than in the earlier situation with the correctly specified forcing. The explanation of this behavior comes from observing the dynamics of the additive bias correction $b(t)$ (Fig. 19, second panel). For both the combined and additive models, $b(t)$ captures the external forcing $f(t)$ that is present in the true signal. Moreover, in the additive model, $b(t)$ also tries to recover the multiplicative part of the noise by adding the high frequency oscillations with frequency ω and large amplitude whenever $\gamma(t)$ takes negative values. On the other hand, the multiplicative model performs poorly—the RMS error is larger than the average observation error, $\sqrt{r^o/2} = 0.063$. There is no means to repair the incorrectly specified forcing by using the multiplicative model. Moreover, the multiplicative model gives the wrong estimation for the damping parameter $\gamma(t)$.

Next, we study how our three filtering models perform, when the external forcing is not specified exactly. Suppose either the amplitude, or the frequency, or the phase of the forcing are unknown, while the remaining two parameters are known. Then, we can vary the unknown parameter around its value in the true signal and study how the filter skill changes. In Fig. 20, we show how the filter skill changes when we vary the amplitude of the forcing A_f (first panel), the frequency of the forcing ω_f (second panel) and the phase of the forcing ϕ_f (third panel), where the forcing has the form

$$f(t) = A_f e^{\mathrm{i}(\omega_f t + \phi_f)}.$$

The true signal was generated with the values $A_f = 1,\ \omega_f = 0.15$, and $\phi_f = 0$. We note that for all three filters and for all three parameters of the forcing, the filters produce the results with the minimum error at the true values of the forcing parameters. Moreover, the filters allow for the variations of the amplitude, A_f, and the phase, ϕ_f, around their respective values in the true signal. However, for SPEKF-M, even slight variations of the frequency, ω_f, lead to the deterioration of the filtered signal with the RMS error greater than the observation error. We also note again that the multiplicative model is not suitable for filtering with incorrect forcing specification. On the other hand both combined and additive models produce the filtered signal with a skill comparable to the skill of the perfectly specified model for various frequencies.

4.5. Summary

From the numerical simulations in this section, we find that SPEKF-C is the method of choice for filtering with model errors since its high filtering skill (nearly as good as the perfectly specified model in many regimes) is robust and the least

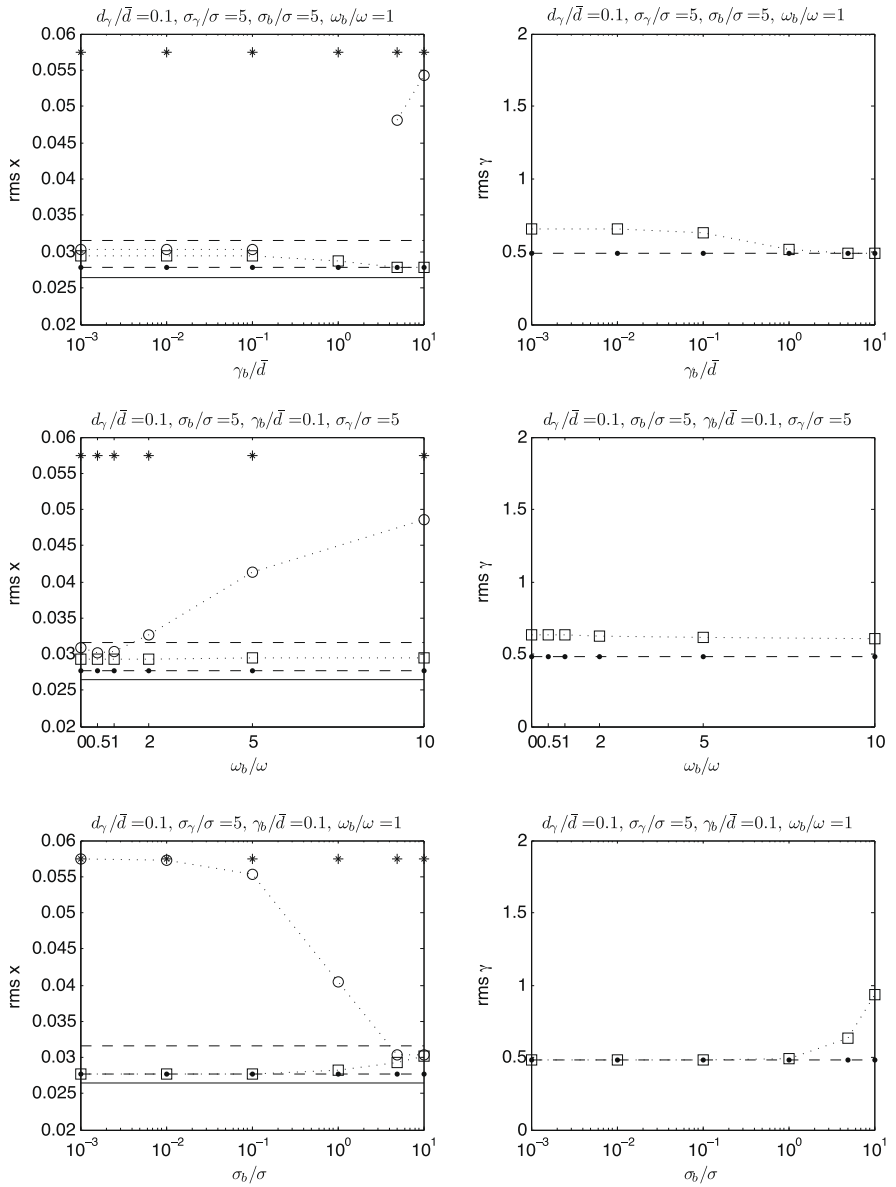

Fig. 18. Forced case: average RMS errors of $x(t) = \mathrm{Re}[u(t)]$ (first columns) and $\gamma(t)$ (second column) as functions of additive stochastic parameters $\{\gamma_b, \omega_b, \sigma_b\}$ for simulations with observation time $\Delta t = 0.25$ and observation noise variance $r^o = 0.25E$. In each panel, we depict the RMS errors for the perfectly specified model (solid), SPEKF-C (square), SPEKF-M (dash-dotted), SPEKF-A (circle), MSM (asterisk), and observation error (dashes).

sensitive to variations of stochastic parameters, observation time, and observation error variance. The simpler strategies (SPEKF-A and SPEKF-M) clearly beat MSM in some parameter regimes and sometimes their skill is as good as or even slightly supersedes the skill of SPEKF-C but they are not as robust as SPEKF-C.

There are extreme parameter regimes in which SPEKF-C is not skillful. In particular, when large damping γ_b is imposed, SPEKF-C behaves exactly like SPEKF-M. Both schemes produce poor filtering skill comparable to MSM when the multiplicative damping d_γ is too strong or when the noise strength σ_γ is too small since the multiplicative bias correction dynamics are nothing more than weak perturbations around the average equilibrium damping, $\bar{d}$, used in MSM. When observation time is beyond the decorrelation time, both schemes also fail for weak damping d_γ (here the multiplicative bias correction term is roughly a Wiener process which has unbounded variance as a function of time) or strong noise σ_γ (too much fluctuation in the OU-process overestimates the multiplicative bias correction term, $\gamma(t)$).

We also note that the advantage of SPEKFs over MSM in addressing the model errors is more significant when regime transitions occur more often. In a numerical study not reported here, we find that all schemes including MSM and the

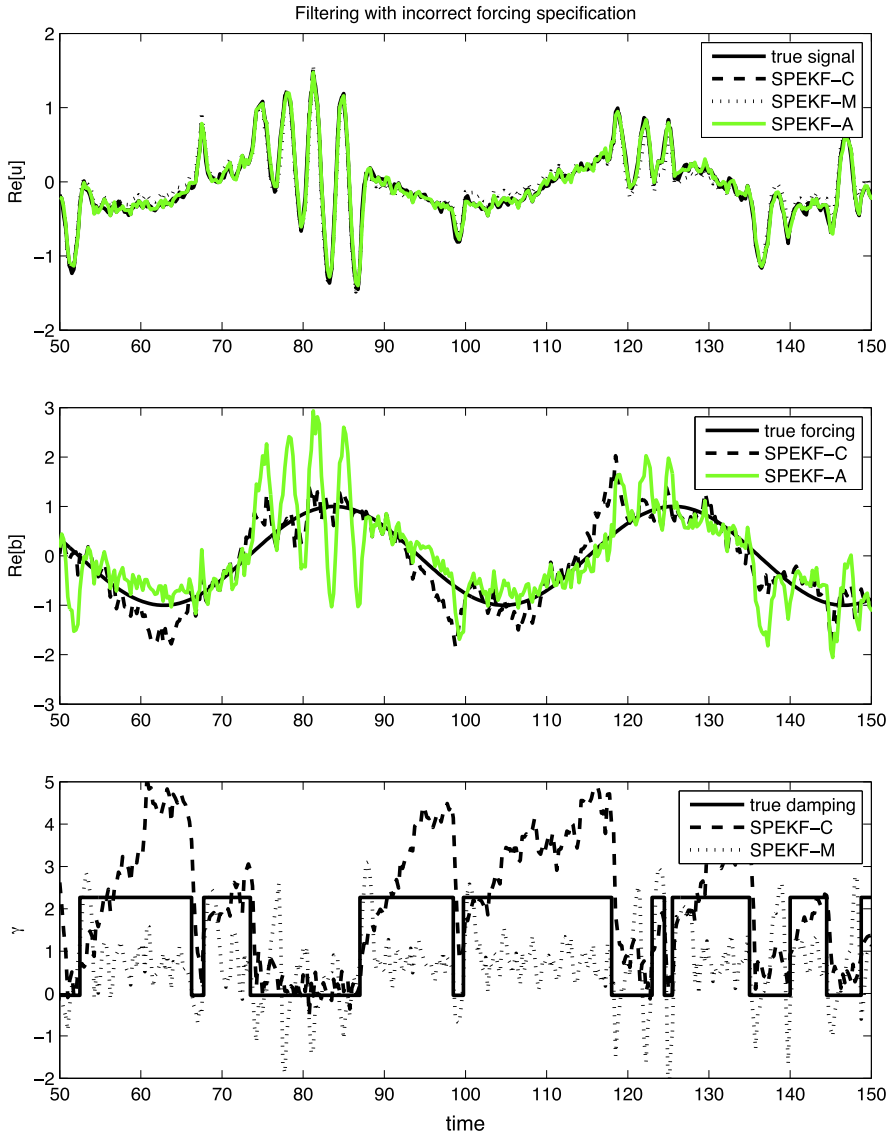

Fig. 19. Filter performance with incorrect forcing specification for $r^o = E$, $\Delta t = 0.25$. The first panel shows $u(t)$ (the true signal is shown with solid black line, SPEKF-C posterior is shown with dashes, SPEKF-M posterior is shown with dots, SPEKF-A posterior is shown with solid grey line), the second panel shows additive bias correction $b(t)$ for SPEKF-C and SPEKF-A together with the true forcing $f(t)$, the third panel shows multiplicative bias correction $\gamma(t)$ for SPEKF-C and SPEKF-M together with the true damping.

perfectly specified model are comparable when the true signal is mostly sitting in the stable regime. This result is understood as follows: when the true signal is in the stable regime, any (discussed) filter model (including MSM) becomes skillful enough to predict noise around zero in the unforced case or around the known forcing.

When the external forcing is unspecified or incorrectly specified, the additive bias correction term $b(t)$ in SPEKF-C and SPEKF-A learns the unknown part of the forcing and the combined and additive models still perform very well with RMS errors comparable to the RMS error of the perfectly specified model. However, the absence of the additive bias correction $b(t)$ in the multiplicative model SPEKF-M prevents this model from being able to filter with incorrect forcing specification.

5. Concluding discussion

In the preceding sections, we developed a suite of stringent test models for improving filtering skill with model errors through systematic stochastic parameter estimation. The key mathematical feature was the development of exact equations

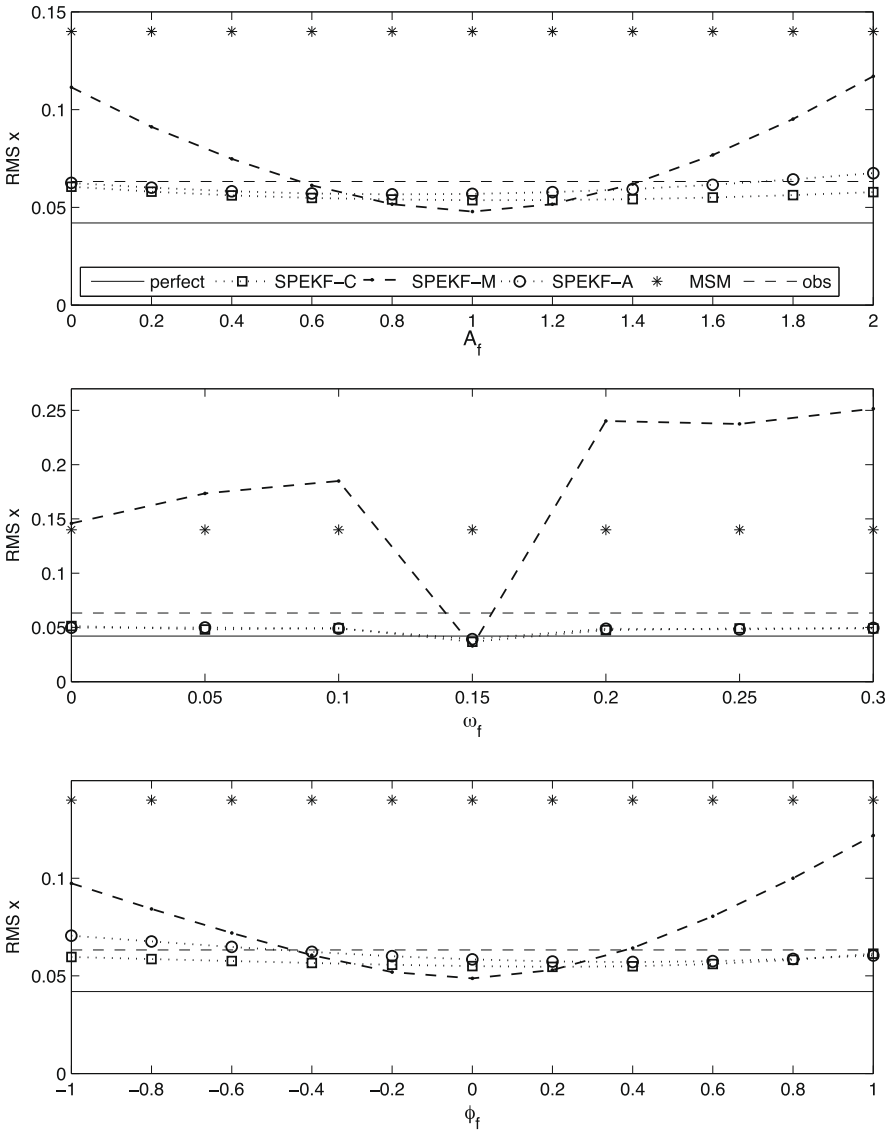

Fig. 20. Filter performance with incorrect forcing specification. The first panel shows the dependence of the RMS error on the forcing amplitude A_f, the second panel on the forcing frequency ω_f, and the third panel on the forcing phase ϕ_f.

for propagation of the mean and covariance which allowed for a suite of SPEKF algorithms for stochastic parameter estimation. In particular, the multiplicative bias term, γ, is assumed to satisfy an OU-process rather than two-state Markov chain process that underlies the dynamics of the true signal. Section 4 contains a comprehensive study of robust parameter regimes for improving filter skill in the presence of significant model error as the observation time, observation noise, and forcing in true signal are varied. Other significant developments in Section 4 included improving the filtering skill even with incorrectly specified forcing and theoretical understanding of the extreme regimes where stochastic parameter estimation fails. It is worth noting here that for turbulent signals that have source terms as in combustion or moist convection, the source terms are often not known precisely so these last results have potential for extensive further development. A more detailed summary of improved filtering skill has already been given at the end of Section 4.

Finally, at first glance, it might seem to the reader that the test models developed here which give useful general insight into stochastic parameter estimation apply only for a complex scalar field. However, two of the authors [22–25] have developed suites of approximate filters with significant skill for filtering turbulent signals with many degrees of freedom based on decoupled Langevin models as in (4); the stochastic parameter estimation algorithms to improve filtering and predictive skill developed here apply directly to these models. These results are presented in a companion article for a prototype filtering problem [26].

Acknowledgments

The research of A.J. Majda is partially supported by the National Science Foundation Grant DMS-0456713, the Office of Naval Research Grant N00014-05-1-0164, and the Defense Advanced Research Projects Agency Grants N00014-07-1-0750 and N00014-08-1-1080. Boris Gershgorin and John Harlim are supported as postdoctoral fellows through the last two agencies.

Appendix A. In this Appendix, we compute the second order statistics of $u(t)$, $\gamma(t)$, and $b(t)$. These analytical formulas are used in the Kalman filter formulation to propagate the posterior covariance from previous analysis to obtain a prior covariance for the next analysis.

A.1. $Var(u(t))$

We compute the variance using

$$Var(u(t)) = \langle |u(t)|^2 \rangle - |\langle u(t) \rangle|^2.$$

In terms of the following notations:

$$u(t) = A + B + C,$$

where

$$A = e^{-J(t_0,t)+\hat{\lambda}(t-t_0)}u_0, \tag{50}$$

$$B = \int_{t_0}^{t} (b(s)+f(s))e^{-J(s,t)+\hat{\lambda}(t-s)}ds, \tag{51}$$

$$C = \sigma \int_{t_0}^{t} e^{-J(s,t)+\hat{\lambda}(t-s)}dW(s), \tag{52}$$

we rewrite

$$\langle |u(t)|^2 \rangle = \langle |A^2| \rangle + \langle |B^2| \rangle + \langle |C^2| \rangle + 2\mathrm{Re}[(A^*B)]. \tag{53}$$

We find the RHS of Eq. (53) term by term

$$\langle |A|^2 \rangle = e^{-2\hat{\gamma}(t-t_0)}(|\langle u_0 \rangle|^2 + Var(u_0) - 4\mathrm{Re}[\langle u_0 \rangle^* Cov(u_0, J(t_0,t))] + 4|Cov(u_0, J(t_0,t))|^2)e^{-2\langle J(t_0,t)\rangle + 2Var(J(t_0,t))},$$

where we used the following property of Gaussian random variables [15,16]

$$\langle zwe^{bx} \rangle = [\langle z \rangle \langle w \rangle + Cov(z,w^*) + b(\langle z \rangle Cov(w,x) + \langle w \rangle Cov(z,x)) + b^2 Cov(z,x)Cov(w,x)]e^{b\langle x \rangle + \frac{b^2}{2}Var(x)}, \tag{54}$$

for complex Gaussian z and w and real Gaussian x.

Next, we have

$$\langle |B|^2 \rangle = \int_{t_0}^{t} ds \int_{t_0}^{t} dr b_{Var}(s,r),$$

where

$$\begin{aligned} b_{Var}(s,r) = {} & e^{-\hat{\gamma}(2t-s-r)+i\omega(r-s)} \times e^{-\langle J(s,t)\rangle - \langle J(r,t)\rangle + \frac{1}{2}Var(J(s,t)) + \frac{1}{2}Var(J(r,t)) + Cov(J(s,t),J(r,t))} \times [(\langle b(s)b^*(r) \rangle - \langle b(s) \rangle [Cov(b^*(r), J(s,t)) \\ & + v(b^*(r), J(r,t))] - \langle b^*(r) \rangle [Cov(b(s), J(s,t)) + Cov(b(s), J(r,t))] + [Cov(b^*(r), J(s,t)) \\ & + v(b^*(r), J(r,t))][Cov(b(s), J(s,t)) + Cov(b(s), J(r,t))]) + f^*(r)(\langle b(s) \rangle - Cov(b(s), J(s,t) \\ & - Cov(b(s), J(r,t))) + f(s)(\langle b(r) \rangle^* - Cov(b(r), J(s,t)^* - Cov(b(r), J(r,t))^*) + f(s)f^*(r) \end{aligned}$$

with

$$\begin{aligned} \langle b(s)b(r)^* \rangle = {} & (1 - e^{\lambda_b(s-t_0)})(1 - e^{\lambda_b^*(r-t_0)})|\hat{b}|^2 + e^{\lambda_b(s-t_0)}(1 - e^{\lambda_b^*(r-t_0)})\hat{b}^* \langle b_0 \rangle + e^{\lambda_b^*(r-t_0)}(1 - e^{\lambda_b(s-t_0)})\hat{b}\langle b_0 \rangle^* \\ & + e^{\lambda_b(s-t_0)}e^{\lambda_b^*(r-t_0)}(Var(b_0) + |\langle b_0 \rangle|^2), + \frac{\sigma_b^2}{2\gamma_b}(e^{-\gamma_b(s+r-2\min(s,r))} - e^{-\gamma_b(s+r-2t_0)})e^{i\omega_b(s-r)}, \end{aligned}$$

$$Cov(b(r), J(s,t)) = \frac{1}{d_\gamma}(e^{-d_\gamma(s-t_0)} - e^{-d_\gamma(t-t_0)})e^{\lambda_b(r-t_0)}Cov(b_0, \gamma_0).$$

We compute the covariance of $J(s,t)$ and $J(r,t)$ for $t_0 \leqslant r \leqslant s \leqslant t$ in the following way:

$$Cov(J(s,t),J(r,t)) = Var(J(s,t)) + Cov(J(s,t),J(r,s)),$$

where

$$\begin{aligned} Cov(J(s,t),J(r,s)) = {} & \frac{Var(\gamma_0)}{d_\gamma^2}(e^{-d_\gamma(t-t_0)} - e^{-d_\gamma(s-t_0)}) \times (e^{-d_\gamma(s-t_0)} - e^{-d_\gamma(r-t_0)}) - \frac{\sigma_\gamma^2}{2d_\gamma^3}(e^{-d_\gamma(t-s)} - e^{-d_\gamma(t-r)} + e^{-d_\gamma(t+s-2t_0)} \\ & - e^{-d_\gamma(t+r-2t_0)} - 1 + e^{-d_\gamma(s-r)} - e^{-2d_\gamma(s-t_0)} + e^{-d_\gamma(s+r-2t_0)}). \end{aligned} \tag{55}$$

In order to find this covariance for $t_0 \leqslant s \leqslant r \leqslant t$, we use the fact that $Cov(J(s,t),J(r,t)) = Cov(J(r,t),J(s,t))$ and follow the same procedure but for s and r switched with each other. Next, we find

$$\langle |C|^2 \rangle = \sigma^2 \int_{t_0}^{t} e^{-2\hat{\gamma}(t-s)} \langle e^{-2J(s,t)} \rangle ds = \sigma^2 \int_{t_0}^{t} e^{-2\hat{\gamma}(t-s)} e^{-2\langle J(s,t)\rangle + 2Var(J(s,t))} ds.$$

Finally, we find

$$\begin{aligned} \langle A^* B \rangle = {} & e^{-\hat{\gamma}(t-t_0)} \int_{t_0}^{t} e^{(\lambda_b - i\omega)(s-t_0) - \hat{\gamma}(t-s)} \langle u_0^* b_0 e^{-J(t_0,t) - J(s,t)} \rangle ds + e^{-\hat{\gamma}(t-t_0)} \int_{t_0}^{t} e^{i\omega(t_0-s) - \hat{\gamma}(t-s)} (\hat{b}(1 - e^{\lambda_b(s-t_0)}) \\ & + f(s)) \langle u_0 e^{-J(t_0,t) - J(s,t)} \rangle^* ds. \end{aligned}$$

where

$$\begin{aligned} \langle u_0^* b_0 e^{-J(t_0,t) - J(s,t)} \rangle = {} & (Cov(u_0^*, b_0^*) + \langle u_0 \rangle^* \langle b_0 \rangle - \langle u_0 \rangle^* [Cov(b_0, J(t_0,t)) + Cov(b_0, J(s,t))] - \langle b_0 \rangle [Cov(u_0, J(t_0,t)) \\ & + Cov(u_0, J(s,t))]^* + [Cov(b_0, J(t_0,t)) + Cov(b_0, J(s,t)] \times [Cov(u_0, J(t_0,t)) + Cov(u_0, J(s,t))]^*) \\ & \times e^{-\langle J(t_0,t)\rangle - \langle J(s,t)\rangle + \frac{1}{2}Var(J(t_0,t)) + \frac{1}{2}Var(J(s,t)) + Cov(J(t_0,t)J(s,t))} \\ \langle u_0 e^{-J(t_0,t) - J(s,t)} \rangle = {} & (\langle u_0 \rangle - Cov(u_0, J(t_0,t)) - Cov(u_0, J(s,t)) \times e^{-\langle J(t_0,t)\rangle - \langle J(s,t)\rangle + \frac{1}{2}Var(J(t_0,t)) + \frac{1}{2}Var(J(s,t)) + Cov(J(t_0,t)J(s,t))} \end{aligned}$$

A.2. $Cov(u(t), u^*(t))$

We use the definition of the covariance to find

$$Cov(u(t), u^*(t)) = \langle u(t)^2 \rangle - \langle u(t) \rangle^2.$$

We find that

$$\langle u(t)^2 \rangle = \langle A^2 \rangle + \langle B^2 \rangle + 2\langle AB \rangle, \tag{56}$$

where we have used the independence of $W(t)$ of other random variables. We find the RHS of Eq. (56) term by term.

$$\langle A^2 \rangle = e^{2\hat{\lambda}(t-t_0)} (\langle u_0 \rangle^2 + Cov(u_0, u_0^*) - 4\langle u_0 \rangle Cov(u_0, J(t_0,t)) + 4Cov(u_0, J(t_0,t))^2) e^{-2\langle J(t_0,t)\rangle + 2Var(J(t_0,t))}.$$

Next, we have

$$\langle B^2 \rangle = \int_{t_0}^{t} ds \int_{t_0}^{t} dr b_{Cov}(s,r),$$

where

$$\begin{aligned} b_{Cov}(s,r) = {} & e^{\hat{\lambda}(2t-s-r)} e^{-\langle J(s,t)\rangle - \langle J(r,t)\rangle + \frac{1}{2}Var(J(s,t)) + \frac{1}{2}Var(J(r,t)) + Cov(J(s,t)J(r,t))} \times [(\langle b(s)b(r) \rangle - \langle b(s) \rangle \times [Cov(b(r), J(s,t)) + Cov(b(r), J(r,t))] \\ & - \langle b(r) \rangle [Cov(b(s), J(s,t)) + Cov(b(s), J(r,t))] + [Cov(b(r), J(s,t)) + Cov(b(r), J(r,t))] \times [Cov(b(s), J(s,t)) \\ & + v(b(s), J(r,t))]) + f(r)(\langle b(s) \rangle - Cov(b(s), J(s,t) - Cov(b(s), J(r,t))) + f(s)(\langle b(r) \rangle - Cov(b(r), J(s,t) \\ & - Cov(b(r), J(r,t))) + f(s)f(r)], \end{aligned}$$

with

$$\begin{aligned} \langle b(s)b(r) \rangle = {} & (1 - e^{\lambda_b(s-t_0)})(1 - e^{\lambda_b(r-t_0)})\hat{b}^2 + e^{\lambda_b(s-t_0)}(1 - e^{\lambda_b(r-t_0)})\hat{b}\langle b_0 \rangle + e^{\lambda_b(r-t_0)}(1 - e^{\lambda_b(s-t_0)})\hat{b}\langle b_0 \rangle \\ & + e^{\lambda_b(s-t_0)} e^{\lambda_b(r-t_0)} \times (Var(b_0) + |\langle b_0 \rangle|^2). \end{aligned}$$

Finally, we find

$$\langle AB \rangle = \int_{t_0}^{t} e^{\hat{\lambda}(2t-s-t_0) + \lambda_b(s-t_0)} \langle u_0 b_0 e^{-J(t_0,t) - J(s,t)} \rangle ds + \int_{t_0}^{t} e^{\hat{\lambda}(2t-s-t_0)} (\hat{b}(1 - e^{\lambda_b(s-t_0)}) + f(s)) \langle u_0 e^{-J(t_0,t) - J(s,t)} \rangle ds.$$

where

$$\begin{aligned}\langle u_0 b_0 e^{-J(t_0,t)-J(s,t)}\rangle = (&Cov(u_0,b_0^*)+\langle u_0\rangle\langle b_0\rangle-\langle u_0\rangle[Cov(b_0,J(t_0,t))+Cov(b_0,J(s,t))]-\langle b_0\rangle[Cov(u_0,J(t_0,t))\\&+Cov(u_0,J(s,t))]+[Cov(b_0,J(t_0,t))+Cov(b_0,J(s,t)]\times[Cov(u_0,J(t_0,t))+Cov(u_0,J(s,t))])\\&\times e^{-\langle J(t_0,t)\rangle-\langle J(s,t)\rangle+\frac{1}{2}Var(J(t_0,t))+\frac{1}{2}Var(J(s,t))+Cov(J(t_0,t)J(s,t))},\end{aligned}$$

A.3. $Cov(u(t),\gamma(t))$

The covariance of $u(t)$ and $\gamma(t)$ is found as follows

$$Cov(u(t),\gamma(t))=\langle u(t)\gamma(t)\rangle-\langle u(t)\rangle\langle\gamma(t)\rangle=\langle u(t)(\gamma(t)-\hat{\gamma})\rangle+\langle u(t)\rangle(\hat{\gamma}-\langle\gamma(t)\rangle)$$

We compute the first term

$$\begin{aligned}\langle u(t)(\gamma(t)-\hat{\gamma})\rangle&=e^{\hat{\lambda}(t-t_0)}\langle u_0e^{-J(t_0,t)}(\gamma(t)-\hat{\gamma})\rangle+\int_{t_0}^{t}e^{\hat{\lambda}(t-s)}\langle(b(s)+f(s))e^{-J(s,t)}(\gamma(t)-\hat{\gamma})\rangle ds\\&=-e^{\hat{\lambda}(t-t_0)}\frac{\partial}{\partial t}\langle u_0e^{-J(t_0,t)}\rangle-\int_{t_0}^{t}e^{\hat{\lambda}(t-s)}\frac{\partial}{\partial t}\langle(b(s)+f(s))e^{-J(s,t)}\rangle ds,\end{aligned}$$

where

$$\frac{\partial}{\partial t}\langle u_0e^{-J(t_0,t)}\rangle=\left[-Cov(u_0,\gamma(t))+(\langle u_0\rangle-Cov(u_0,J(t_0,t)))\times\left(\hat{\gamma}-\langle\gamma(t)\rangle+\frac{1}{2}\frac{\partial}{\partial t}Var(J(t_0,t))\right)\right]\times e^{-\langle J(t_0,t)\rangle+\frac{1}{2}Var(J(t_0,t))}$$

and

$$\begin{aligned}\frac{\partial}{\partial t}\langle(b(s)+f(s))e^{-J(s,t)}\rangle=\Bigg[&-Cov(b(s),\gamma(t))+(\langle b(s)\rangle+f(s)-Cov(b(s),J(s,t)))\\&\times\left(\hat{\gamma}-\langle\gamma(t)\rangle+\frac{1}{2}\frac{\partial}{\partial t}Var(J(s,t))\right)\Bigg]e^{-\langle J(s,t)\rangle+\frac{1}{2}Var(J(s,t))}.\end{aligned}$$

The derivative of $Var(J(s,t))$ with respect to t has the following form:

$$\frac{\partial}{\partial t}Var(J(s,t)=-\frac{1}{d_\gamma^2}(\sigma_\gamma^2(e^{-d_\gamma(t-s)}-1)+(\sigma_\gamma^2-2d_\gamma Var(\gamma_0))\times(e^{-d_\gamma(t+s-2t_0)}-e^{-2d_\gamma(t-t_0)})).$$

A.4. $Cov(u(t),b(t))$

We have

$$Cov(u(t),b(t))=\langle u(t)b^*(t)\rangle-\langle u(t)\rangle\langle b(t)\rangle^*.$$

We find

$$\begin{aligned}\langle u(t)b^*(t)\rangle=\langle u(t)\rangle\hat{b}^*(1-e^{\lambda_b^*(t-t_0)})+e^{(\hat{\lambda}+\lambda_b^*)(t-t_0)}\langle u_0b_0^*e^{-J(t_0,t)}\rangle+e^{\lambda_b^*(t-t_0)}\int_{t_0}^{t}e^{\hat{\lambda}(t-s)}\langle b_0^*b(s)e^{-J(s,t)}\rangle ds+e^{\lambda_b^*(t-t_0)}\\\times\int_{t_0}^{t}e^{\hat{\lambda}(t-s)}f(s)\langle b_0e^{-J(s,t)}\rangle^*ds+\frac{\sigma_b^2}{2\gamma_b}\int_{t_0}^{t}e^{-\langle J(s,t)\rangle+\frac{1}{2}Var(J(s,t))}e^{(-\hat{\gamma}+i(\omega-\omega_b))(t-s)}\times[e^{-\gamma_b(t-s)}-e^{-\gamma_b(s+t-2t_0)}]ds,\end{aligned}$$

where

$$\langle b_0e^{-J(s,t)}\rangle=(\langle b_0\rangle-Cov(b_0,J(s,t)))e^{-\langle J(s,t)\rangle+\frac{1}{2}Var(J(s,t))}$$

$$\begin{aligned}\langle u_0b_0^*e^{-J(t_0,t)}\rangle=(&Cov(u_0,b_0)+\langle u_0\rangle\langle b_0\rangle^*-\langle b_0\rangle^*Cov(u_0,J(t_0,t))-\langle u_0\rangle Cov(b_0,J(t_0,t))^*+Cov(u_0,J(t_0,t)Cov(b_0,J(t_0,t))^*)\\&\times e^{-\langle J(t_0,t)\rangle+\frac{1}{2}Var(J(t_0,t))}\end{aligned}$$

$$\begin{aligned}\langle b_0^*b(s)e^{-J(s,t)}\rangle=(&e^{\lambda_b(s-t_0)}Var(b_0)+\langle b(s)\rangle\langle b_0\rangle^*-\langle b_0\rangle^*Cov(b(s),J(s,t))-\langle b(s)\rangle Cov(b_0,J(s,t))^*\\&+Cov(b(s),J(s,t)Cov(b_0,J(s,t))^*)\times e^{-\langle J(s,t)\rangle+\frac{1}{2}Var(J(s,t))}\end{aligned}$$

A.5. $Cov(u(t),b^*(t))$

We have

$$Cov(u(t),b^*(t))=\langle u(t)b(t)\rangle-\langle u(t)\rangle\langle b(t)\rangle$$

We find

$$\langle u(t)b(t)\rangle = \langle u(t)\rangle\hat{b}(1-e^{\lambda_b(t-t_0)}) + e^{(\hat{\lambda}+\lambda_b)(t-t_0)}\langle u_0 b_0 e^{-J(t_0,t)}\rangle + e^{\lambda_b(t-t_0)}\int_{t_0}^{t} e^{\hat{\lambda}(t-s)}\langle b_0 b(s) e^{-J(s,t)}\rangle ds + e^{\lambda_b(t-t_0)}\int_{t_0}^{t} e^{\hat{\lambda}(t-s)} f(s)\langle b_0 e^{-J(s,t)}\rangle ds,$$

where

$$\langle u_0 b_0 e^{-J(t_0,t)}\rangle = (Cov(u_0, b_0^*) + \langle u_0\rangle\langle b_0\rangle - \langle b_0\rangle Cov(u_0, J(t_0,t)) - \langle u_0\rangle Cov(b_0, J(t_0,t)) + Cov(u_0, J(t_0,t) Cov(b_0, J(t_0,t))) \times e^{-\langle J(t_0,t)\rangle + \frac{1}{2}Var(J(t_0,t))}$$

$$\langle b_0 b(s) e^{-J(s,t)}\rangle = (e^{\lambda_b(s-t_0)} Cov(b_0, b_0^*) + \langle b(s)\rangle\langle b_0\rangle - \langle b_0\rangle Cov(b(s), J(s,t)) - \langle b(s)\rangle Cov(b_0, J(s,t)) + Cov(b(s), J(s,t) Cov(b_0, J(s,t)) \times e^{-\langle J(s,t)\rangle + \frac{1}{2}Var(J(s,t))}$$

References

[1] J.J. Tribbia, D.P. Baumhefner, The reliability of improvements in deterministic short-range forecasts in the presence of initial state and modeling deficiencies, Monthly Weather Review 116 (1988) 2276–2288.
[2] E.J. Pitcher, Application of stochastic dynamic prediction to real data, Journal of the Atmospheric Sciences 34 (1) (1977) 3–21.
[3] J.L. Anderson, An adaptive covariance inflation error correction algorithm for ensemble filters, Tellus A 59 (2007) 210–224.
[4] S.-J. Baek, B.R. Hunt, E. Kalnay, E. Ott, I. Szunyogh, Local ensemble Kalman filtering in the presence of model bias, Tellus A 58 (3) (2006) 293–306.
[5] J.A. Carton, G. Chepurin, X. Cao, A simple ocean data assimilation analysis of the global upper ocean 1950-95. Part I: Methodology, Journal of Physical Oceanography 30 (2000) 294–309.
[6] D.P. Dee, R. Todling, Data assimilation in the presence of forecast bias: the GEOS moisture analysis, Monthly Weather Review 128 (9) (2000) 3268–3282.
[7] D.P. Dee, A.M. Da Silva, Data assimilation in the presence of forecast bias, Quarterly Journal of the Royal Meteorological Society 124 (1998) 269–295.
[8] J. Ching, J.L. Beck, K.A. Porter, Bayesian state and parameter estimation of uncertain dynamical systems, Probabilistic Engineering Mechanics. 21 (1) (2006) 81–96.
[9] R. Ghanem, M. Shinozuka, Structural system identification I: theory, Journal of Engineering Mechanics-ASCE 121 (2) (1995) 255–264.
[10] B. Friedland, Treatment of bias in recursive filtering, IEEE Transactions on Automatic Control AC-14 (1969) 359–367.
[11] B. Friedland, Estimating sudden changes of biases in linear dynamical systems, IEEE Transactions on Automatic Control AC-27 (1982) 237–240.
[12] A.H. Jazwinski, Stochastic Processes and Filtering Theory, Academic, San Diego, California, 1970.
[13] B.D. Anderson, J.B. Moore, Optimal Filtering, Prentice-Hall, Englewood Cliffs, NJ, 1979.
[14] C. Chui, G. Chen, Kalman Filtering, Springer, New York, 1999.
[15] B. Gershgorin, A.J. Majda, A nonlinear test model for filtering slow–fast systems, Communications in Mathematical Sciences 6 (3) (2008) 611–649.
[16] B. Gershgorin, A.J. Majda, Filtering a nonlinear slow–fast system with strong fast forcing, Communications in Mathematical Sciences, in press.
[17] A.J. Majda, R.V. Abramov, M.J. Grote, Information theory and stochastics for multiscale nonlinear systems. CRM Monograph Series, vol. 25, American Mathematical Society, Providence, Rhode Island, USA, 2005.
[18] T. Delsole, Stochastic model of quasigeostrophic turbulence, Surveys in Geophysics 25 (2) (2004) 107–149.
[19] R. Salmon, Lectures on Geophysical Fluid Dynamics, vol. 378, Oxford University Press, 1998.
[20] A.J. Majda, M.J. Grote, Explicit off-line criteria for stable accurate time filtering of strongly unstable spatially extended systems, Proceedings of the National Academy of Sciences 104 (2007) 1124–1129.
[21] J. Pedlosky, Geophysical Fluid Dynamics, Springer, New York, 1979.
[22] E. Castronovo, J. Harlim, A.J. Majda, Mathematical criteria for filtering complex systems: plentiful observations, Journal of Computational Physics 227 (7) (2008) 3678–3714.
[23] J. Harlim, A.J. Majda, Mathematical strategies for filtering complex systems: regularly spaced sparse observations, Journal of Computational Physics 227 (10) (2008) 5304–5341.
[24] J. Harlim, A.J. Majda, Filtering nonlinear dynamical systems with linear stochastic models, Nonlinearity 21 (6) (2008) 1281–1306.
[25] J. Harlim, A.J. Majda, Catastrophic filter divergence in filtering nonlinear dissipative systems, Communications in Mathematical Sciences in press.
[26] B. Gershgorin, J. Harlim, A.J. Majda, Improving filtering and prediction of sparsely observed spatially extended turbulent systems with model errors through stochastic parameter estimation, Journal of Computational Physics, submitted for publication.
[27] A. Bensoussan, Stochastic Control of Partially Observable Systems, Cambridge University Press, 2004.
[28] C.W. Gardiner, Handbook of Stochastic Methods for Physics, Chemistry, and the Natural Sciences, Springer-Verlag, New York, 1997.
[29] R.E. Kalman, R. Bucy, A new results in linear prediction and filtering theory, Transactions of the ASME, Journal of Basic Engineering 83D (1961) 95–108.
[30] G. Lawler, Introduction to Stochastic Processes, Chapman & Hall/CRC, 1995.